Humidity's effect on strength and stiffness of containerboard materials

A study in how the relative humidity in the ambient air affects the tensile and compression properties in linerboard and fluting mediums

Fukts inverkan på wellpappsmaterials styrka och styvhet

Frida Strömberg

Faculty of Health, Science and Technology

Department of Engineering and Chemical Science, Chemical Engineering, Karlstad University

Master Thesis, 30hp

Supervisors: Helena Håkansson (KaU), Christophe Barbier and Sara Christenson (BillerudKorsnäs)

Examiner: Lars Järnström

2016-06-15

Serial number

Abstract

The aim of this thesis was to investigate the difference between containerboard materials strength and stiffness properties in tension and compression, how the mechanisms behind compressive and tensile properties are affected by the relative humidity of the ambient air and how the relative humidity affects the compressive response of the fibre network. These properties are used to predict the lifetime performance of corrugated boxes and to prevent early collapses of the boxes and thereby waste or harm of the transported goods inside. The work also discusses the methods used to evaluate the different properties and how reliable the results are. The experimental part includes testing of linerboard and fluting materials from both virgin and recycled fibres, which have been conditioned at 50% and 90% relative humidity. The compression tests were filmed to evaluate if different compression failure modes can be related to the strength and stiffness of the material. The results indicated that the compressive strength and stiffness differ from the strength and stiffness values in tension at 90% relative humidity. Compressive strength is lower in both 50% and 90% relative humidity compared with the tensile strength. However, the compression stiffness shows a higher value than the tensile stiffness at 90% relative humidity. The study of the method for evaluating the compressive behaviour of the paper does not present a complete picture on what type of failure the paper actually experience.

Executive summary

The purpose of this study was to evaluate the compressive and tensile properties as well as the relation between properties at different climates for the materials used in containerboard, study the different failure mechanics that occur in short span compression testing and investigate how moisture affect these mechanics. The differences between the methods used to evaluate the compressive and tension properties were also studied.

Commercial containerboard is used all over the world to transport food and other fragile goods. It is therefore important to be able to predict the performance of the boxes. This is done by simulating boxes with computer software based on the tension and compressive abilities of the containerboard materials; linerboard and fluting. An objective in this study was to evaluate if all parameters need to be experimentally evaluated or if the parameters can be calculated.

The study consists of a laboratory study which included several different paper materials; White Kraft Liner, N/S fluting, Brown Kraft Liner, Test Liner and Recycled Medium ranging between 100-180 g/m^2. All materials were tested for the strength and stiffness properties in both compression and tension at 50% RH and 90% RH.

The method used to determine the compression strength and stiffness was the Short Span Compression Test (SCT). The testing procedure was recorded to be able to determine what type of failure the samples experienced as well as if the stiffness and strength value of the failure could be related to a certain type of failure.

During the SCT measurements it became apparent that the machine does not evaluate the compression in the paper. A new method for evaluating the SCT force strain curve had to be used to be able to compare the compression stiffness against the tensile stiffness, as well as the retention of the stiffness and strength values at 90% RH.

In addition to the testing of the compressive behaviour in the paper a relative humidity study was conducted. Saturated salt solutions were used to acquire different levels of RH in which papers was conditioned to be able to determine the moisture content in the fibre networks. SCT specimens were conditioned at the different levels of RH to evaluate the compressive response in the paper depending on the moisture content.

When studying the retention of the stiffness and strength properties for the two different methods the results in this study show that there are small differences between the different materials in both tension and compression. These results can however only be related to the paper itself as the results from the absolute strength and stiffness values show a clear advantage of the virgin based materials and grammages.

The influence of the humidity in the paper affected the paper differently in tension and compression. At 90% RH, the strength values of the materials all dropped to about 50% of the original strength at 50% RH, with tensile strength showing higher values than the compressive strength. When comparing the stiffness properties however, the compression stiffness for all the virgin based materials, in both MD and CD, and some of the recycled materials was higher than the tensile stiffness of the paper network. This can be related to the differences in the testing methods as the SCT's stiffness values are more dependent on the fibres compared to tension which depend on the fibre network.

When evaluating the recorded material from the SCT measurements, the results showed that the four different types of failure modes occurs at both 50% and 90% RH with no clear shift towards a specific

type of failure. For the majority of the paper studied, the most occurring failure was a global bending failure. The different kinds of failure do however not correspond to the strength or stiffness in the materials, which is good for the everyday industrial testing of paper materials. It does, however, not give a true prediction of the compressive strength and stiffness properties of the paper.

In the relative humidity study all materials showed an increase of the moisture content as a function of the relative humidity, leading to a decrease of the compressive strength in the paper. The values from the study resemble a mirrored adsorption curve for water vapour when plotted against the relative humidity in which the samples were conditioned.

To summarize the findings of this report there is differences between the different mechanics in compression and tension. Due to the differences the fibre network responds differently to the influence of moisture. Virgin based linerboard and fluting is stronger and stiffer than recycled fibres at higher RH, which is important to keep in mind when choosing the components for the containerboard.

The mechanisms behind the different failures differ, in tension properties depend on the fibre network while the compression failure depend on the strength and stiffness of the fibres in the network. As the recordings showed, global bending failures of the sample can occur in the compression measurements, presenting a false compressive strength of the paper.

Acknowledgments

This thesis was conducted between January 2016 to June 2016 in cooperation between Karlstad University and BillerudKorsnäs.

I would like to extend special thanks to and show my gratitude for my supervisors Christophe Barbier, Helena Håkansson and Sara Christenson for their support and guidance throughout this thesis.

I also wish to thank Hanna Larsson and Patrik Svärd at BillerudKorsnäs for their assistance with the experimental works and equipment throughout the study, as well as the people located in the R&D office for their help and useful discussions.

Lastly I want to express my thanks to my supportive family and friends who kept me company throughout the evenings and weekends.

Abbreviations

A	Area [m^2]
α	Take-up factor
α_{SCT}	Rescaling factor for SCT
α_f	Bonded area between fibres per kilo [m^2/kg]
A_w	Water activity
b	Width of a test piece [mm]
BKL	Brown Kraft liner
C	Guggenheim's constant
CD	Cross direction
d	Thickness [µm]
E	Specific elastic modulus [MNm/kg]
E_C^x	Compression stiffness, *x* represents the RH
E_C^b	Compression stiffness [kN/m]
E_C^w	Compression stiffness index [MNm/kg]
E_{SCT}^x	SCT stiffness, *x* represents the RH
E_T^x	Tensile stiffness, *x* represents the RH
E_S^b	Tensile stiffness [kN/m]
E_T^w	Tensile stiffness index [MNm/kg]
ε_T	Tensile strain at break [%]
ε_C	Compression strain at break [%]
F	Force [N]
F_T	Force at break [N]
SCT	Short span Compression Test
K	Factor depending on bulk properties of water
l	Average Fibre length [m]
L	Lumen
$L_{fluting}$	Length of fluting
L_{Liner}	Length of linerboard
MD	Machine direction
Medium	Recycled medium
ML	Middle lamella
M_o	Moisture content of a monolayer
N/S	Neutral Sulphite Semi-Chemical
ρ	Density (kg/m^3)
P	Primary wall
σ_T^b	Tensile strength [kN/m]
σ_T^w	Tensile strength index [kNm/kg]
σ_{ZS}^w	Zero span tensile strength index [Nm/kg]
σ_C^b	Compression strength [kN/m]
σ_C^w	Compression Strength index[MNm/kg]
Sx	Secondary wall, x represent the different layers
τ_T	Fibre-fibre bond Shear stress at failure [kN/m]
TL	Test liner
ZD	Z-direction
w	Grammage [g/m^2]
WTKL	White top Kraft liner

Table of Contents

1. Introduction 1
   1.1. Background 1
   1.2. Problem formulation 1
   1.3. BillerudKorsnäs 2
2. Theory 3
   2.1. Paper as a material 3
      2.1.1. Fibre's components and structure 3
      2.1.2. Virgin fibres 6
      2.1.3. Recycled fibres 7
   2.2. Pulping and Papermaking processes 7
      2.2.1. Kraft pulping 7
      2.2.2. NSSC pulping 8
      2.2.3. Recycled fibre process 8
      2.2.4. The paper machine 9
   2.3. Mechanical properties of corrugated board 11
      2.3.1. Tensile strength and stiffness 12
      2.3.2. Compression strength and stiffness 14
   2.4. Influence of humidity on compression and tensile properties 16
3. Experimental 19
   3.1. Material 19
      3.1.1. Conditioning of samples at 50% RH 20
      3.1.2. Conditioning and preparation of samples at 90% RH 20
   3.2. Laboratory study 21
      3.2.1. Grammage, thickness and density 21
      3.2.2. Anisotropy 22
      3.2.3. Tensile properties 22
      3.2.4. Compression properties 22
      3.2.5. Visual recording of SCT test 23
      3.2.6. STFI Short span compression tester. 23
   3.3. Determination of moisture content in paper 25
4. Results and discussion 27
   4.1. Stiffness and strength retention at 90%RH 27
      4.1.1. Linerboard 27
      4.1.2. Fluting 31

4.1.3. Influence of humidity on the stiffness in paper. 33
4.2. Compression properties 34
4.2.1. The compression failure mechanism vs. the tensile failure mechanism 34
4.2.2. SCT Failure modes at 50% RH and 90% RH 35
4.2.3. SCT Correlation between failure modes and the strength/stiffness of the material 38
4.3. Influence of humidity 40
4.3.1. Grammage, thickness and density 40
4.4. Determination of the moisture content in paper and the effects on SCT performance 42
5. Conclusion 44
5.1. Principal findings 44
5.2. Future works 44
6. References 46
Appendix I A1
Appendix II A2
Appendix III A7

1. Introduction

1.1. Background

With the increase of goods on the global trade market, often combined with long transporting chains, the demands for light and strong packages constantly increase. Lighter packages to reduce the transportation costs and stronger products that can withstand changing climates to minimize the damage of for example fruit and vegetables. The majority of packages used in transporting today are made from corrugated board, which are made up of liner and a corrugated medium.

As the packages often are stacked and transported between different climates it is important for the corrugated board to be able to withstand the changes in humidity to prevent a collapse of the structure that will damage the content. For this purpose virgin fibre corrugated board has shown to be superior to an equal box made from recycled liner and fluting. (BillerudKorsnäs, 2016).

BillerudKorsnäs is a producer of bleached primary kraft liner and N/S Fluting that is used in containerboard. To further help and invent better product and package solutions for customers they also offer a service called managed packaging, where a team of packaging designers and engineers work together to present new solutions based on fibrous materials. They use the Billerud Box Design software (BBD) that helps them to simulate how well a package will perform over time and in different climates, commonly 50% and 90% relative humidity (RH). The software requires values for the tensile strength, tensile stiffness, compression stiffness and compression strength in 50% and 90%. All parameters can be determined experimentally but it requires intensive testing. Therefore a question rises about if all parameters need to be measured or if there is a relationship between the values in tension and compression and between the values in different climates. In order to investigate which parameters need to be measured and how to measure them, the following problem have been formulated.

1.2. Problem formulation

The objective of this thesis can be divided into three different sections:

- Study the mechanisms for collapse/rupture of containerboard experiencing compressive or tensile loads. Is there a difference between the mechanisms and how do they differentiate from one another?
- Investigate the methods used today to evaluate compression and tensile properties in fibrous materials to evaluate if the performances of the methods deliver reliable results for testing in climates with higher relative humidity than 50%.
- Investigate how the moisture content in the containerboards components changes at different relative humidity levels in the surrounding air and how the relative humidity affects the compressive behaviour of the containerboard.

The study was limited to uncoated commercial paper constituting the components in corrugated board, based both on virgin and recycled wood fibres. Only the standard methods for evaluating compression and tensile properties of the fibrous network were used. Behaviour over time (creep) is an important topic for true performance of corrugated boxes. Nevertheless, due to the time limit of the thesis creep was not evaluated nor discussed

1.3. BillerudKorsnäs

BillerudKorsnäs is one of the world leading suppliers of primary based packaging materials. The company was formed 2012 when the two companies Billerud and Korsnäs merged together. With its three business areas; Consumer Board, Packaging Papers and Corrugated Solutions spread out over eight production units. The main office is located in Solna and together with numerous customer service and sales offices all over the world BillerudKorsnäs challenges the conventional packaging for a sustainable future.

At Gruvön Mill in Grums, paper products made from 100% virgin fibres are produced on 5 machines. Gruvön Mill produces a wide range of different products based on bleached kraft- and NSSC pulp.

The business areas also provides customer service in managed packaging and have two special laboratories located at Gruvöns mill, BoxLab and PackLab. The engineers work with evaluating existing box and bag designs to be able to optimize and present newer and better solutions for their customers. In addition BoxLab includes a climate chamber which makes it possible to study boxes and box components performances when exposed to extreme climates.

2. Theory

2.1. Paper as a material

Paper is a material that in most cases is based on wood but can also be based on other plants such as grass or cotton. This study will focus on the wood based paper. Wood based fibres can be divided into two different groups; Hardwood and softwood. Softwood fibres come from coniferous trees such as pine and spruce while hardwood is broad-leaf trees e.g. birch, eucalyptus and acacia. *(Daniel. 2009)*

Depending on the species of coniferous trees the fibres can be between 2.8-7.2 mm long and have a fibre width of 27-65 µm. Hardwood fibres are both shorter and slimmer ranging between 0.8-1.3 mm in length and a diameter of 14-28 µm *(Retulainen et al. 1998).*

2.1.1.Fibre's components and structure

The fibre structure can be divided into three main organic components; cellulose, hemicellulose and lignin. In addition there are also small parts of inorganic compounds present called extractives. Together these compounds build up the fibres in a layered structure that is similar to fibre reinforced composite materials *(Kolseth and de Ruvo 1986).*

2.1.1.1. Cellulose

Cellulose is made from glucose molecules bonded with 1→4 β-glycosidic bonds and form long unbranched polysaccharide chains with high degrees of polymerisation with values over 15000. It constitutes approximately 40-50% of the dry mass of the fibres and works as the "skeleton" which contribute to the stiffness and strength of the wood. The structure of cellulose can be seen in *fig. 2.1. (Kolseth and de Ruvo 1986.)*

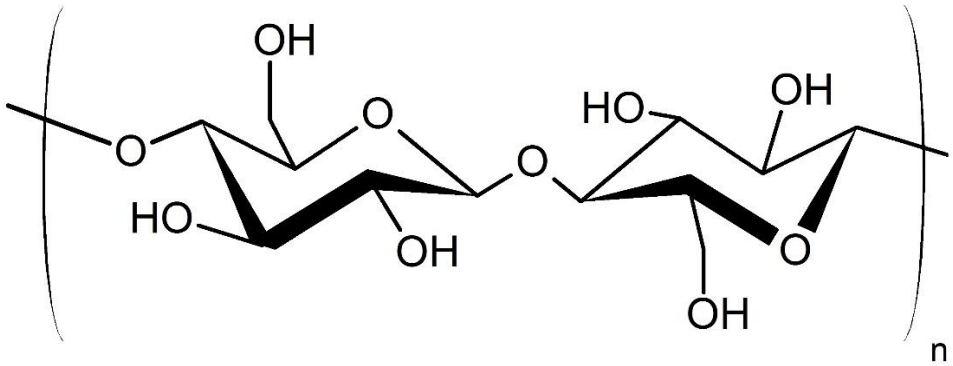

Figure 2.1. The primary structure of the cellulose chain. The figure was created in ChemSketch.

Due to structure of the cellulose chains, they can be packed tightly together and form a highly crystalline 3D structure called elementary fibrils. The structure is distinctive due to the different bonds found in each dimension. In the first dimension, the backbone of the cellulose chain is bonded with covalent glycosidic bonds and enforced with hydrogen bonds creating a straight and stable structure. Hydrogen bonds between separate cellulose chains make up the second dimension forming sheets of chains. The sheets are then stacked on top of each other and thus creating the third dimension. In the third dimension the sheets are held together due to Van der Waals- and χ- interactions bridges *(Lennholm and Henriksson 2009).* Normally a cellulose chain is about 5-7 µm in length, but due to the stacking in the higher dimensions the chains will overlap and the fibrils can become over 40 µm long. The average elementary fibril contains 36 cellulose chains and form bundles with other

elementary fibrils to form micro-fibrils and later macro-fibrils that builds up the fibre walls of the tree *(Daniel 2009, Lennholm and Henriksson 2009).*

2.1.1.2. Hemicellulose

Hemicellulose surrounds the cellulose micro-fibrils to form a structural support in the cell walls. Hemicellulose is similar to the cellulose chains in that they are long polysaccharide chains, but the main chain can be built from several different kinds of monosaccharides e.g. glycose, mannose, galactose and/or xylose. Hemicellulose also hold multiple side groups and have significantly lower degree of polymerisation (around 200) compared to cellulose, making the hemicellulose chains much shorter. *(Teleman A. 2009, Sjöström E. 1981)*

Due to its less linear structure the hemicellulose can only form semi-crystalline structures, usually without hydrogen bonds. The hemicellulose can be found between the cellulose micro-fibrils in the cell walls and the surrounding lignin matrix. The function of hemicellulose is not completely understood but some suggestions is support the cellulose fibres by keeping the micro-fibrils in a separated order to regulate the porosity and strength of the fibre walls. *(Teleman A. 2009)*

There are different types of hemicellulose and the structures of the chains also depend on different side groups and the wood specie. The hemicellulose contribute to regulate the moisture content of the wood as hemicellulose can bind more water than both cellulose and lignin. Common types of hemicellulose in softwood are arabinoglucurono-xylan (7-15% of the total dry mass of hemicellulose), galacto-glucomannan 10-15% and glucomannan (5-8%). Hardwood normally holds about 15-35% glucuronoxylan with small parts of glucomannan (2-5%). *(Teleman A. 2009)*

2.1.1.3. Lignin

Lignin is a large amorphous organic polymer present in the wood fibres. The component acts as a glue that bind cellulose and hemicellulose with hydrogen bonds to form a stiff and hard network. Due to lignin's hydrophobic abilities it serves to make the cell walls of the fibres waterproof and thereby prevents swelling of the hemi- and cellulose polymers. Finally the lignin serves as a protection against microorganisms that would otherwise consume the polysaccharide chains within the cell walls. *(Henriksson 2009, Sjöström 1981)*

Lignin is one of the most complex structures out of all natural biopolymers. With its building blocks connected by ether bridges and carbon-carbon bond lignin forms a large random three dimensional web with no apparent start or stop, making it impossible to calculate the compounds molecule weight. An example of the most common compounds in lignin is illustrated in *Fig 2.2*. *(Henriksson 2009, Sjöström E. 1981)* The amount of lignin present in the wood differs between hardwood and softwood with the former containing about 20% lignin and the later between 15-35%. *(Henriksson 2009)*

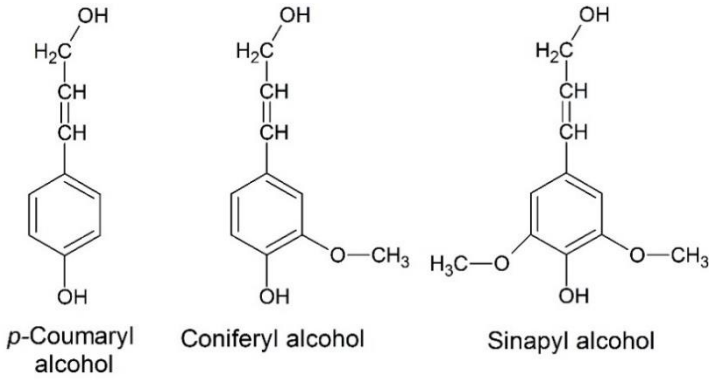

Figure 2.2. Three of the most common building blocks of lignin.

2.1.1.4. Cell wall structure

The wall structure of the fibre cells is built up by the compounds described in section 2.1.1.1-2.1.1.3 and illustrated in *Fig 2.3*. The middle lamella (ML) surrounding the structure and the primary wall (P) are made up of mostly lignin and residue hemicellulose also known as pectic compounds. The primary wall is built up from randomly orientated microfibrils and is very thin compared to the secondary wall and along with the middle lamella removed during pulping. These two layers act at the concrete between the fibre cells. *(Daniel 2009, Henriksson 2009)*

The second wall is made up from three layers; S1, S2 and S3, where S2 is the thickest out of the three, making out 80-90% of the entire cell wall. In S1 and S3, microfibrils are orientated at angles >50° spiralling around the cells lumen (L). The angle of the microfibrils present in the S2 layer holds a smaller angle of 10-30° and is a major contributor to the tensile stiffness and tensile strength of the fibre. Worth mentioning is that the model described above is just one out of several. Some models consider the S3 layer as a tertiary wall instead. (*Daniel 2009, Bristow and Kolseth 1986)*

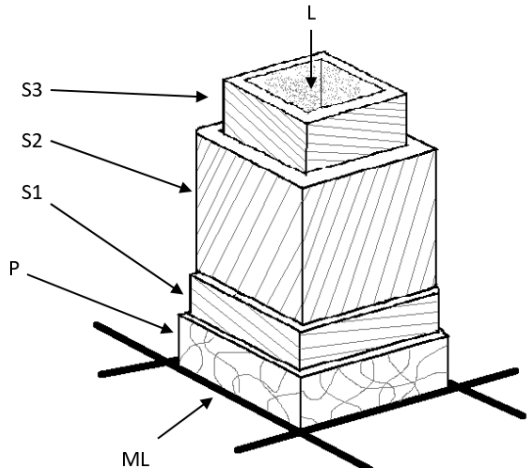

Figure 2.3. A schematic view of the different layers of a fibre cell wall redrawn from Bristow and Kolseth (1986). ML = middle lamella, P = primary wall, S1, S2 and S3 = different layers of the secondary wall and L = Lumen. The angle of the microfibrils in each layer is illustrated by the grey lines.

All different layers are composed from cellulose, hemicellulose and lignin, but the ratio between the three is different depending on which part of the wall is studied. As mentioned in an earlier section the primary wall and middle lamella hold high contents of lignin (about 55-60% of the total amount of lignin). *(Eklund and Lindström 1991).* The cellulose present in the primary wall has low degrees of polymerisation and is tangled in a random pattern. *(Daniel 2009)*

The secondary wall contains more cellulose and hemicellulose than the primary wall and middle lamella and the majority resides in the thicker S2 layer. Common for all three layers is that the cellulose is ordered in a crystalline pattern with hemicellulose and lignin as an intermediate. There are several models describing how the arrangements of the three main components within the wall layers are arranged. In *Fig 2.4* three different models summarized and discussed by Daniel are presented. (2009).

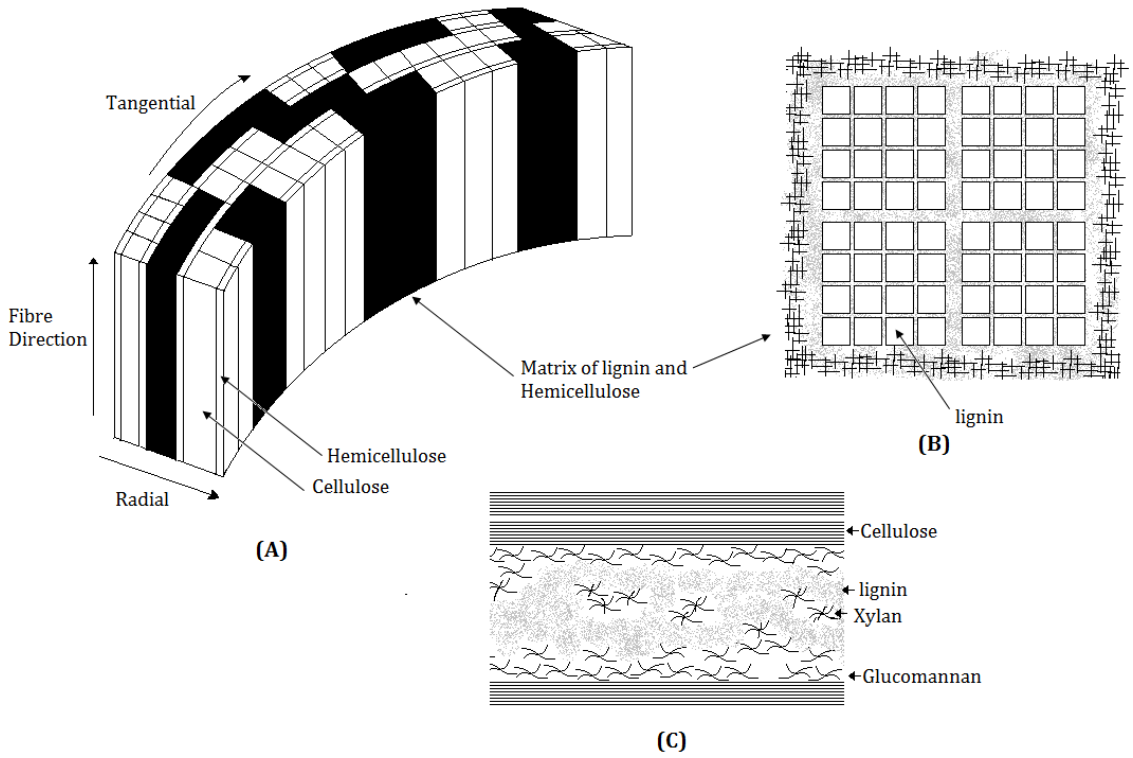

Figure 2.4. Illustrate 3 different models of how the lignin, hemicellulose and cellulose are organised in the cell wall. Redrawn from Daniel (2009).

Model A and B resembles one another in the way that microfibrils are clustered together into larger aggregations and surrounded by a lignin/hemicellulose matrix. Model C differs from the other two in the way that they differentiated different types of hemicellulose suggesting that glucomannan is bounded in closer proximity to the cellulose microfibrils than xylan which is found embedded in the surrounding lignin. *(Daniel 2009).*

2.1.2. Virgin fibres

Virgin fibres are types of fibres that come from processing of wood. Depending on how the fibres have been processed there are significant differences between the paper properties of the end product. Chemical pulps have fibres that are slim and have low contents of lignin and hemicellulose making them more flexible and ductile. Chemical pulping does not shorten the wood fibres which result in longer fibres then mechanical pulps (depending on the wood species). Mechanical pulp fibres are stiffer, as most of the lignin remains in the cell walls and the pulp contains more fines. The fines are a result of small parts of the fibre walls being ripped away during the refining of the wood *(Retulainen et al. 1998)*. N/S Fibres are a combination of the chemical and mechanical fibre due to the N/S pulping process, see section 2.2.2. N/S fibres are “half cooked”, which implies that the lignin matrix between

the fibres has been softened by the cooking process and is easy to separate with mechanical defibrillation. This result pulps containing in long, stiff fibres with low contents of fines.

Before the paper machine the fibres go through refining where the fibres experience internal and external fibrillation. Internal fibrillation is a result of delamination between the layers of the fibre wall and improves the conformability, swelling and flexibility of the fibres. *(Lindström 1986)*

Swelling in the fibre wall causes an increase of the total surface areas of fibre, facilitating the collapse of the fibres and increases the available bonding area on the fibre. External fibrillation improves the strength of the inter fibre bonds further by tangling together when the fibres still reside in a water suspension. As the water is removed during the drying process of the paper, the external fibrils will retract to the fibre's surface and effectively binding the fibres together. The effects that are more prominent in chemical pulps compared to mechanical pulp due to the lower lignin content. *(Retulainen et al. 1998).*

2.1.3. Recycled fibres

Fibres that have gone through a drying process and then recycled experience hornification. It is the process of when the porous structure of the fibre wall close irreversibly when the fibre fibrils bind to the fibre surface, causing stiffening of the fibres polymer chains. An effect of the closure of the pores in the fibre walls is the reduced swelling ability in the fibres, causing reduced bonding abilities. *(Zhang et al. 2001, Lindström 1986).* Recycled fibres are also shorter then virgin fibres due to refining. Refining of the recycled fibre is important because it reverses some of the hornification effects on the fibre surface, recovering parts of the fibres porous structure and of the microfibrils that helps to increase the fibres number of bonding sites. Chemical treatment and addition of strength agents will also help the recycled fibres to retain more strength in a fibrous web. *(Zhang et al. 2001)*

2.2. Pulping and Papermaking processes

To be able to produce paper of any sort, the wood fibres need to be separated from each other. This can be done by several different mechanical processes e.g. ground-wood pulp (GWP), thermo mechanical pulping (TMP) and Chemical thermo mechanical pulping (CTMP) which all separate the fibres by mechanical work. These processes have high yield (>95%) due to most of the incoming material remaining in the pulp *(Höglund 2009).* Another way to separate the fibres is by cooking them with chemicals. Sulphite pulping, Neutral sulphite semi chemical pulping and kraft pulping, (which is the dominant method used globally), are all examples of chemical pulping (*Brännvall 2009b)*. In the chemical processes the lignin and parts of the hemicellulose in the middle lamella and primary wall are softened and dissolved by chemicals which leaves a lower yield of the pulp (depending on type of wood, cooking temperature and time *(Gellerstedt 2009)*. Paper does not have to come from a primary raw material like wood but can also be produced from recycled paper materials. In Europe, about 54 % of the produced products from the paper industry are based on recycled fibre materials. In the production of corrugated boxes, 90% of the raw materials are recycled fibres *(ERPC, 2016).*

2.2.1. Kraft pulping

The aim of the chemical pulping is to separate the fibres and remove large quantities of lignin. In the Kraft pulping, wood chips are first impregnated with and cooked under pressure in an aqueous alkali mixture called white liquor, composed of sodium hydroxide (NaOH) and sodium sulphide (Na_2S), at temperatures between 150-170°C (*Brännvall 2009b).* Impregnation of the wood chips is done to get

an even distribution of the cooking chemicals and thus get an homogeneous cook and reduce shives in the pulp. During the cooking process the pH varies between 14 (at the beginning) to 12.5 at the end and can be carried out with both hardwood as well as softwood and generate a pulp yield of around 45-50% *(Sjöström 1981, Brännvall 2009b).*

As the white liquor dissolves the components by breaking ether bridges within the structure of the wood, mostly in lignin and hemicellulose compounds, the residues are dissolved in the cooking liquor, which adopts a dark brown/black colour or black liquor. The black liquor is then recycled back into white liquor which make the process economically sustainable as the process generates energy that is recycled into the mill as steam and electricity *(Brännvall 2009b, Sjöström 1981).*

After the cooking process, the fibres are washed and can then be used for production of brown kraft paper products or be furthered processed by removing additional lignin in a bleaching process producing bleached kraft pulp. Kraft pulp are used in a large quantity of different paper products e.g. liner, sack paper and liquid board *(Brännvall 2009b).*

2.2.2. NSSC pulping

NSSC pulping is a variant of the sulphite cooking process but has a pH ranging within 7-9. Combined with mechanical processing of the pulp, the pulp is usually used for producing fluting. The neutral pH spares much of the hemicellulose which contributes to the stiffness of the fibres, a mechanical property valued for corrugated board *(Gullichbsen & Fogelholm 2000).* Thin hardwood chips are impregnated with steam and neutral sulphite pulping liquor and partially digested to soften the lignin-cellulose matrix to make it easy to refine the pulp. The refining is done in two steps, with the first being defibration of the softened wood chips before the pulp is washed. After washing, the pulp goes through refining to further separate the fibres and improve the ability to create bonds sites in a fibre network to increase the strength properties *(Dahlgren et al. 1980).*

Since the duration of the cooking phase is short, NSSC pulps have a high yield of stiff and strong fibres suitable for corrugated boards. Birch is one of the most used hardwood types for NSSC fluting due to its high cellulose content. To improve the runnability on the paper machine, softwood fibres are mixed in the NSSC pulp *(Gullichbsen & Fogelholm 2000, Bränvall 2009b).*

The recycled of the cooking liquor from a NSSC cook can be fed into the stream of black liquor from the Kraft process.

2.2.3. Recycled fibre process

Recycled fibres can come from a wide range of different fibrous materials. Office waste material, magazines and old corrugated containers are just a few examples. The fibres can be made from never recycled products or products already made from recycled fibres. A fibre can be recycled between 5-7 times before it "falls" out of the recycling process *(Engstrand and Johansson 2009).*

At first the recovered paper is pulped and goes through several steps to remove impurities from the pulp such as ink, plastic materials, metal and coating. Ink can be removed in two different processes where the first is washing of the pulp. During the washing process the smaller ink particles are separated from the fibres through a metal wire screen. The second process, floatation, uses the difference in electrochemical properties between the ink and the fibres. The pulp has a small air bubbles pouring through in which the small ink particles is trapped. As the bubbles rise to the surface, foam is formed which can carefully be removed *(Engstrand and Johansson 2009).*

Larger particles are separated from the pulp by using screening and centrifugal separation. In the screening process, particles larger than the fibres are removed, e.g. coating residue and plastic. In the centrifugal separation step, particles are removed by difference in density, for example metal parts *(Engstrand and Johansson 2009).*

Depending on the end use of the pulp, it can be bleached to accompany the demands of the final product. Pulp used for newspaper and tissue products are bleached while fibres used for corrugated board can be used without the bleaching step *(Engstrand and Johansson 2009).*

2.2.4. The paper machine

The majority of fibrous material products are produced on a paper/board machine. There is a large amount of different shapes and sizes of machines, but in general they are all made up of the same parts. *Fig. 2.5* gives an overview of a paper machine.

A paper machine can be divided into two sections; wet end and dry end. The wet end can further be separated into the headbox, wire and press section. Before the pulp reach the machine's headbox it goes through the stock preparation, where it is refined and diluted to a slurry of ~0.6% solid content. Depending on what type properties that are desired in paper, additional chemicals can be mixed into the slurry, e.g. retention aids, dry strength agents such as starch or fillers, which improves the optical properties. *(Brännvall 2009a)*

The pressurised headbox distributes an even layer of the fibre suspension onto the wire section as well as to prevent flocculation of the fibres within the slurry. A machine can have multiple headboxes or one headbox designed to create a layered structure with different properties of the layer, e.g. a dense and strong top layer suited for printing and a bulky bottom layer for high bending stiffness.

As the slurry is distributed over the forming wire the paper fibres align in the machine direction due to a speed difference between the headbox and the wire. As the fibre slurry leaves the headbox shearing forces align the fibres in the MD before they hit the wire. The function of the wire is to dewater the paper distributed over the wire surface as well as further improve the formation of the paper web. As the water is removed from the web, shearing forces further "combs" the fibres in the machine direction and contribute to an anisotropic structure of the paper web. *(Norman 2009)*

At the first part of the wire, water is removed with gravity and foil elements, which create vacuum below the wire "sucking" water out of the web. Further down the wire, suction boxes remove additional water up to a dry solid content in the paper around 20%, at which the web is strong enough to support itself and is carried over to the press section. *(Norman 2009)*

In the press section the paper web pass 2-4 press nips, which together with two press felts mechanically press water out of the paper web until it reaches a dry solid content of 40-50%. The pressing of the paper changes the density of the web and correlates to the strength properties of the finished paper. Both tensile and compression properties increase by wet pressing, while the bending stiffness decrease due to the reduced thickness of the web. *(Norman 2009)*

After the press section, the paper web is transferred into the drying section consisting of multiple heated cylinders, which removes remaining water in the web. *(Brännvall 2009a)*

The paper web then passes through two calendar rolls, which evens out variations in the grammage, decrease the thickness of the paper and smoothen out the surface of the paper for improved surface

properties. The finished paper is wound up on reel for further handling. Not all types of paper need to be calendered. *(Brännvall 2009a)*

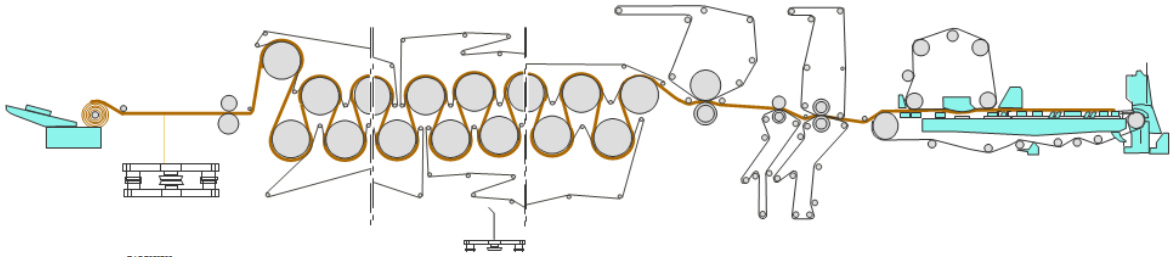

Figure 2.5. Schematic view over a paper machine that can produce two layered linerboard. Parts from right to left: headbox and wire section, pressing section, drying section, calendar nip and reel section. With permission from BillerudKorsnäs.

Due to the way paper is produced on the machine, paper has 3 distinguishable principal directions; machine direction (MD), cross machine direction (CD) and the out-of-plane direction (ZD). The orientation of fibres in paper lies in the MD-CD plane, with the majority of fibres aligned in MD, creating anisotropic sheets. Paper is therefore a heterogeneous material with multiple variables contributing to the mechanical properties, e.g. strength and stiffness properties are higher in MD while the strain at break is higher in CD *(Fellers 2010, Rigdahl and Hollmark 1986).* Since this study is concentrated on linerboard and fluting qualities, the products based on these qualities will be in focus.

2.2.4.1. Containerboard products.

Some products that are easy to find in the nearest store are corrugated board, paperboard and tissue. Both corrugated board and paper board are used for packages. Paperboard is normally found in the food sector as milk containers or cereal boxes. Corrugated board is more adapted for transport, as the requirements on strength and stiffness performances are higher *(Söremark and Tryding 2009).*

Corrugated board is a material that is built up from liner and fluting, with liner being the top and bottom layers and a core of fluting being the wavy middle layer. Liner is made up from two layers which hold different properties. The base layer contributes to tensile strength and stiffness of the board. On top of the base layer there is a thin top layer composed of fibres which hold a high fine content to get a smoother surface suited for printing *(Brännvall 2009b).* The function of fluting is to separate the two liner layers and to have good resistance agains compression, resulting in a sturdy construction of the corrugated board. The structure (illustrated in *Fig. 2.6*) is an adaptation of the engineering beam theory used in solid mechanics. The corrugated board is approximated as flat panels separated by a rigid core, similar to an I-beam. The stucture improves the bending stiffness for the board but reduces the material needed for the board basic weight low *(Söremark and Tryding 2009).*

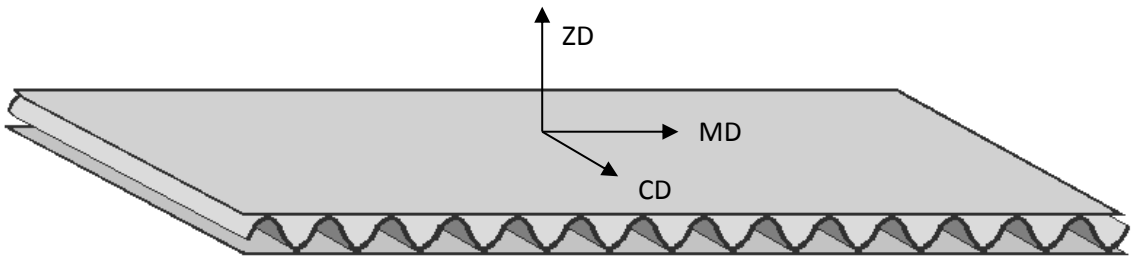

Figure 2.6. The structure of corrugated board. The top and bottom layers are made from linerboard and the core is made from fluting.

Fluting and liner are converted into corrugated board in a corrugator. First, liner and fluting are unwound from reels. The fluting passes two heated corrugator cylinders which give the fluting the characteristic wavy appearance. Glue made from starch is added to the tops of the corrugated fluting before being pressed against the liner. The type of fluting is determined by the height, wavelength and the number flutes per meter. Table 2.1 present the standardised types of fluting, though small differences can be found between different containerboard produces. *(Söremark and Tryding 2009, Grafiska Yrkesnämden 1983).*

Table 2. 1. Flute types.

Flute type	Wave Height [mm]	Number of waves/m
A	4.8	110
C	3.6	130
B	2.4	150
E	1.2	290
F	0.7	350
G &N	0.5	550

From the profile a take-up factor can be calculated by

$$\alpha = \frac{L_{lFluting}}{L_{lLiner}}, \alpha > 1. \quad [1]$$

A multilayerd containerboard can be composed from multipe flute types, depending on the needs of the end user.

2.3. Mechanical properties of corrugated board

An aim of this study was to evaluate how the compression and tensile properties' of the components correlate to the performance of the boxes. It is important to understand the connection between the experimental performance and the theoretical performance, predicted by the BBD software, of the boxes. A common way to evaluate the corrugated performance is through a box compression test (*BCT).* To be able to predict the *BCT* performance, without having to test a large amount of boxes a formula known as McKee's formula is frequently used *(Eq. 2).* McKee's formula combines the Edge crush test (*ECT*), the bending stiffness of the panels and the design of the box, to predict a BCT value *(Frank 2014).*

$$BCT = 2.028 \cdot ECT^{0.746} (\sqrt{S_{MD} \cdot S_{CD}})^{0.254} \cdot Z^{0.492} \quad [2]$$

Where *BCT* is the calculated compression strength of the box, *ECT* is the compression strength of a corrugated board panel, S_{MD} and S_{CD} are the bending stiffness's in their corresponding directions of the panel and *Z* is a parameter that describes the dimensions of the box. The model is derived from the panel buckling theory combined with empirical relations between the strength of the box panel and the instability of the panel. As *Eq. 2* indicates, the performance of the panel contributes to the performance of the finished box design. The boards compression stiffness are related the physical parameters from the liner and medium (*Frank 2014).*

ECT has been shown to correlate to other compression tests, e.g. the compression strength values from the short compression test (*SCT*) *(Dimitrov and Heydenrych, 2009).* The relation shown in *Eq. 3* is used to calculate the *ECT* value from the *SCT* values for the components of the corrugated board.

$$ECT = \left(\sum SCT_{liner} + \alpha SCT_{Fluting}\right) \quad [3]$$

Where α is the take-up factor for the fluting profile.

The bending stiffness of the corrugated panels is also a contributing factor to the box performance. Bending stiffness is the part of the McKee formula that is derived from the laminate theory and stands in relation to the thickness and stiffness of the board (*Frank 2014, Kajanto 1998).*

Because the performance of a corrugated box can be related to both tensile and compression properties of the base materials, the importance of how the mechanics of the two properties proceeds is essential. One of the objectives in this study is therefore to evaluate if different mechanics governs the strength and stiffness properties in tension and compression. In everyday testing of fluting materials, it is only the CD direction that is evaluated for its mechanical properties. This is due to the converting process which results in the wavers of the fluting being aligned in CD. For this study, however, the strength and stiffness properties is evaluated for both MD and CD, as they are used for the geometric mean value in McKee's formula.

Compression and tensile strength and stiffness are affected by the density of the sheet network, which correlates to how well-bonded the fibre network is. The density is affected by the pulping process, refining and wet pressing of the network, fine content and additives. *SCT* is however not as dependent of the degree of bonding of the fibres as tensile strength. In addition, *SCT* have been suggested to correlate to the geometry of the fibres. *(Fellers and Gimåker 2011, Wink et al, 1984, Shallhorn et al. 2004, Niskanen and Kärenlampi 1998).* Wahlström reported that the restrained drying of the paper web affects the tensile strength positively, due to an increase of load bearing fibres in the network *(Wahlström 2010).*

2.3.1. Tensile strength and stiffness

Tensile strength of the paper is governed by the failure of fibre-fibre bonds in the network. Rupture of fibres can occur in well-bonded sheets. Page's theory for tensile strength is one of the most accepted, presented in *Eq. 4.*

$$\frac{1}{\sigma_T^w} = \frac{9}{8} \cdot \frac{1}{\sigma_{ZS}^w} + \frac{12}{\tau_s l \alpha_f} \quad [4]$$

Where $\sigma_T{}^w$ is the tensile strength index, $\sigma_{zs}{}^w$ is the zero span tensile strength index of the fibres, l is the average fibre length, α_f represent the bonded area between fibres per kg and τ_T is the shear stress at failure of a fibre-fibre bond. But due to the stochastic behaviour of the fibre-fibre interactions and different process parameters Page's theory describes ideal cases. The theory gives a good approximation of the tensile strength index in paper dried under restraint. *(Fellers 2010, Page 1969)*

Tensile strength of a well-bonded fibrous network is approximately 1/3 of a fibre's tensile strength *(Rigdahl and Hollmark 1986, Fellers 2010, Räsisänen et al. 1996).* Failure in a fibrous network occurs when the bonding sites slip due to shear stress. Page's theory suggests that increased load will continue to increase until a critical point at which the network breaks. Up to this point the network will experience elastic and plastic deformation. An example can be seen in *Fig 2.7.*

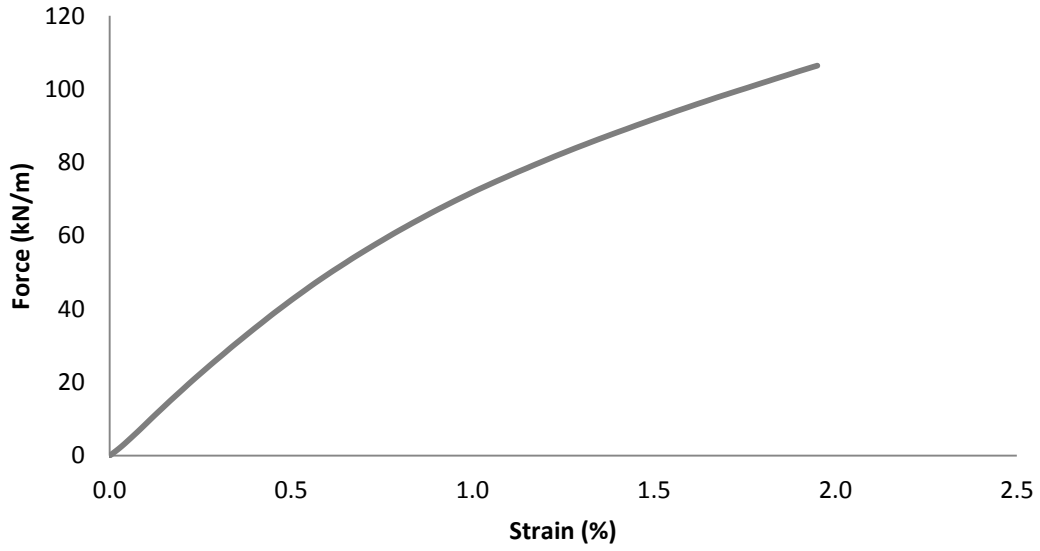

Figure 2.7. Example of a force-strain curve for N/S Fluting.

The stress-strain curve is acquired by measuring the increase of the load and the elongation of the test sample. Tensile strength is evaluated as the point of maximum force distributed over a unit area and the method is standardised in ISO 1924-3:2011. As paper is a compressible material, the area of the cut surface can vary, and instead the tensile strength is calculated as the force per width, as defined by *Eq. 5 (Fellers 2010, Levlin 1999).*

$$\sigma_T^b = \frac{F_T}{b} \qquad [5]$$

σ_T^b represents the force per width in the sample (kN/m), F_T is the force (N) at critical failure and b corresponds to the width (mm) of the paper strip. Because paper comes in many different qualities the tensile strength is normalised against the grammage of the sample to be able to compare results, see the modified versions of *Eq. 5'*.

$$\sigma_T^w = 1000 \cdot \frac{F_T}{b \cdot w} \qquad [5']$$

Where σ_T^w is the indexed strength on the sample and w is the grammage (g/m^2) of the sample. The value is multiplied with 1000 to get the strength in kNm/kg *(Fellers 2010, Levlin 1999).*

Tensile stiffness of the fibre network is evaluated from the linear part of the stress strain curve. *(ISO 1924-3:2011, Räisänen et al. 1996).* As the fibre network is exposed to external loads the stress will become distributed over the entire network and is affected by the formation of the fibre network. Under a constant load there are fibres that are inactive, meaning some fibres carry higher loads then others. This is because of the shapes of the fibres. Free segments between the fibre bonds can be curly resulting in an inactive fibre. A fibre network with poor formation will experience high levels of local stress *(Niskanen and Kärenlampi 1998, Fellers 2010)*. As the load increases the number of activated fibres in the network, elastic deformation occurs in the fibre-fibre bonding sites. At a given yield point the bonds will start to deform plastically. The tensile stiffness is defined up to yielding point and can be derived from Hooke's Law (*Räisänen et al. 1996).* The tensile stiffness for elastic materials such as paper is defined according to *Eq. 6.*

$$E_T^b = \frac{E_T}{b} \quad [6]$$

Where the E_T^b is the tensile stiffness for the paper, *T* represents tension and can be replaced with C to indicate compression stiffness. E_T represents the initial slope of the force-strain curve and *b* is the width of the sample. *(Fellers 2010).*

The tensile stiffness for paper is indexed against the grammage by

$$E_T^w = 1000 \cdot \frac{E_S^b}{w} \quad [7]$$

and is reported in Nm/kg. When indexing both tensile strength and tensile stiffness against the grammage, the used grammage is for paper conditioned at 50% RH to make the results easier to compare.

2.3.2. Compression strength and stiffness

The stress and strength relation described in tensile by *Eq 5, 5'* and *6* applies to the compression strength and stiffness properties as well. Comparing tensile- and compression strength and stress strain curves, the strain at break for the web is significantly lower and a typical stress-strain curve can be seen in *Fig 2.8. (Gunderson et al. 1988, Chalmers 1998 and Fellers and Gimåker 2011).* However multiple authors state that the elastic modulus of the fibre network remains the same in compression and tension. *(Fellers and Gimåker 2011, Mäkelä 2010, Kajanto 1998, Fellers 1986)*

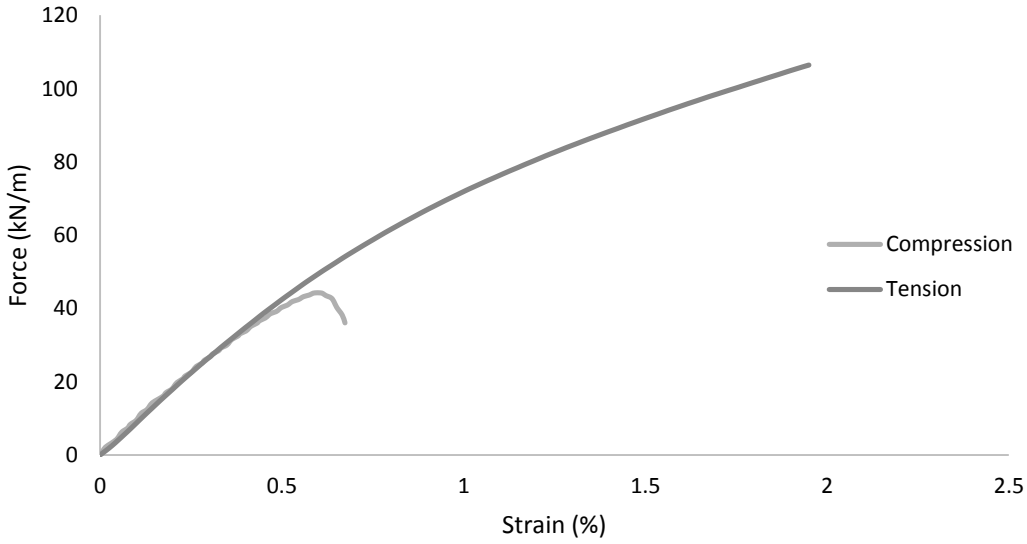

Figure 2.8. A force-strain curve in compression and in tension. The compression stress strain curve has been inverted to illustrate the similarity between the stiffnesses.

In a pure compression failure, loading forces in the sample continue to increase and the amount of load bearing fibres in the network increase. In early stages the increase of the loading strain is proportionally distributed among the fibre segments and appears as the linear part of the stress strain curve. Further increase of the strain causes the fibres to deform due to instabilities in the cell wall which lead to local buckling of the fibre walls and or the free fibre segments in bending or shear modes. At the point of failure in the sheet a certain amount of fibres have yielded and elastic energy is

released which causes the network a shear dislocation in the ZD direction *(Fellers 1986, Fellers and Gimåker 2011).*

Failure mechanisms in compressive load are still a discussed area with no complete theory of what happens in the fibres. Some suggestions are that compression failure occurs by local buckling of the fibres, delamination of the fibre walls and shear failure between the external fibre bonds. When buckling occurs the compression stress is converted into bending, which abruptly decreases the load capacity of the fibre *(Fellers and Gimåker 2011, Kajanto 1998).* Delamination of the fibre walls reduces the carrying capacity of the fibres to a greater degree than buckling. The delamination between fibres and within the wall structure causes a decrease of the local thickness, which affect the bending stiffness. The loss of local bending stiffness results in local buckling (*Kajanto 1998).* Information on which type of failure mode would correspond to a stronger fibre and fibre network is absent in the literature studied.

2.3.2.1. Short span compression test

There are several different methods for determine a papers compressive strength, e.g., Ring crush test (*RCT*) or Corrugated crush test (*CCT*). Both these methods are a combination of buckling failures and compression failures and a new method was sought after that could better evaluate the true compression of the paper. A method was developed in the early 1980s that evaluated the compression strength over a very short span, effectively preventing buckling in the sample. The method was called short span compression test (*SCT*) and is today widely accepted over the world. (*Fellers and Gimåker 2011).*

SCT is a basic set up of two pair of clamps placed 0.7 mm apart. A sample is placed between the clamps as seen in *Fig 2.9.* The clamps press down on the sample with a force of 2300 ± 500 N to prevent sliding, then starts to approach each other with a strain rate of 429%/min, simulating a buckling failure for a beam with fixed ends. As the stress in the sample reaches the point of failure the sample can express three different kinds of failure modes, illustrated in *Fig. 2.10 (ISO 9895:2009, Hansson 2013)*. Hansson also observed a forth failure mode, in which no visible failure can be seen in the due to that the sample glided between the machine clamps. According to Fellers and Gimåker (2011) the most common failure of the sample is an asymmetrical failure due to shear stress in the paper, which is supported by Hagman et al. (2013).

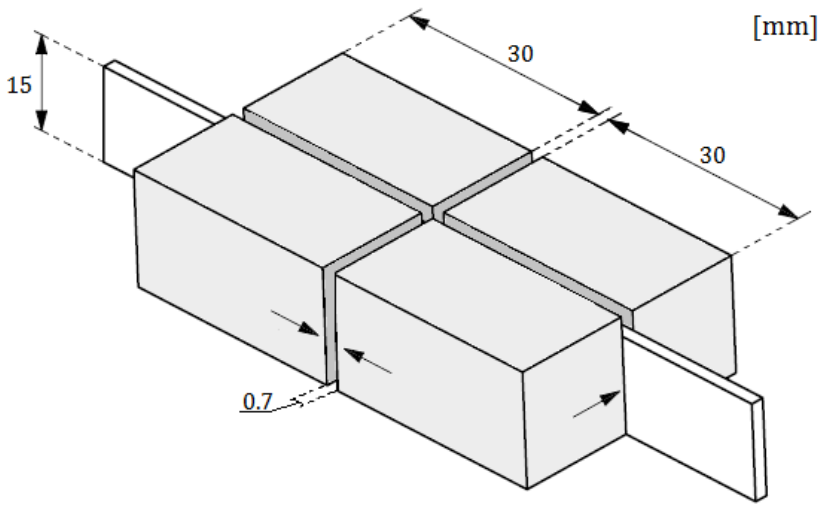

Figure 2.9. a schematic setup of the short compression strength tester, arrows indicating how the clamps move. Redrawn from ISO 9895:2009.

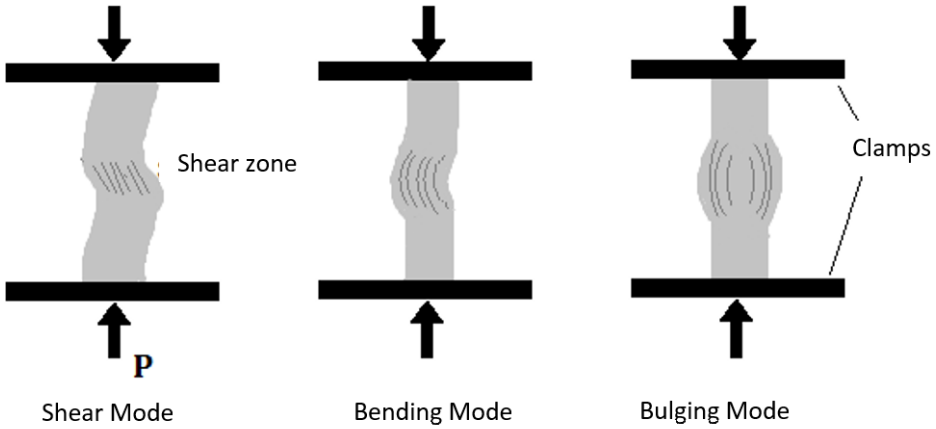

Figure 2.10. Illustration of the 3 different failure modes observed in SCT. Inspired by Kajanto 1998.

SCT is not as dependent on the degree of bonding of the fibres as tensile strength. This is due to the 0.7 mm span between the clamps, which is shorter than the mean length of hardwood fibres *(Retulainen et al. 1998).* In addition, *SCT* have been suggested to correlate to the geometry of the fibres *(Fellers and Gimåker 2011, Wink et al, 1984, Shallhorn et al. 2004)*. On the other hand, the moisture content of the sample affects the performance in compression, causing the strength to decrease *(Fellers and Bränge 1985).* Results from the SCT method have been shown to have better correlation to the ECT of corrugated board panels compared to RCT or CCT. ECT is used to predict the performance of the panels in corrugated boxes. (*Fellers and Gimåker 2011).*

Due to the short free length span in the SCT method, the compression strength can be misleading for the performance of the paperboard *(Mäkelä 2010).* Because of the short span between the clamps the length-thickness ratio will result in a low slenderness ratio which is used in Euler's buckling failures. In more realistic situation several orders of magnitudes will separate the length and thickness resulting in high values on the slenderness ratio (*Fellers and Gimåker 2011).* As the *SCT* failure mode can be of the bending nature, the *SCT* value does not truly represent the compression strength of the paper, but it is however useful for product control *(Mäkelä 2010).* An alternative method for testing the compression stiffness and strength of the paper is by using the long compression span test (LCT).

In the LCT method the distance between the clamps is 78 times that of the distance between the SCT clamps and uses a wider test piece of 25 mm (15 in SCT). To support the sample and prevent it from buckling the LCT method is equipped with columns evenly spread out over the length of the sample. Needles placed along the middle of the paper allow the method to acquire a complete force-strain curve. Mäkelä (2010) studied the relation between the LCT and SCT and showed that a correlation between the two methods exists, with SCT giving of stronger values compared to LCT. LCT is however not available for commercial uses and will therefore not be included in this study *(Hagman et al. 2013, Mäkelä 2010).*

2.4. Influence of humidity on compression and tensile properties

Moisture from the ambient air affects the mechanical properties of fibrous materials. As the moisture content in paper increases, causing a decrease in the strength and stiffness properties (both for compression and tension), strain at break increases *(Chalmers 1998, Page 1969, Back et al. 1983, Fellers and Bränge 1985).* The moisture content in the paper is related to the relative humidity (RH)

of the surrounding air. As corrugated board is used for transportation of goods, the material will experience changes in the RH. RH is dependent on the temperature and as the temperature drops the RH increase. For food packages which usually are stored in cold climates it is therefore important that the material can withstand the changes in the RH. At standard conditions (23°C±1°C and 50%±2% RH) the moisture content in linerboard is measured to be about 6.0- 7.5%. *(Markström 1999)*

Another influence on the performance of the paper is the RH history. The paper binds or release water molecules depending on the amount of water in the ambient air and the temperature. Depending on the moisture history in the paper, the water molecules will experience adsorption or desorption. The two different sorption processes can be seen in *Fig 2.11*.

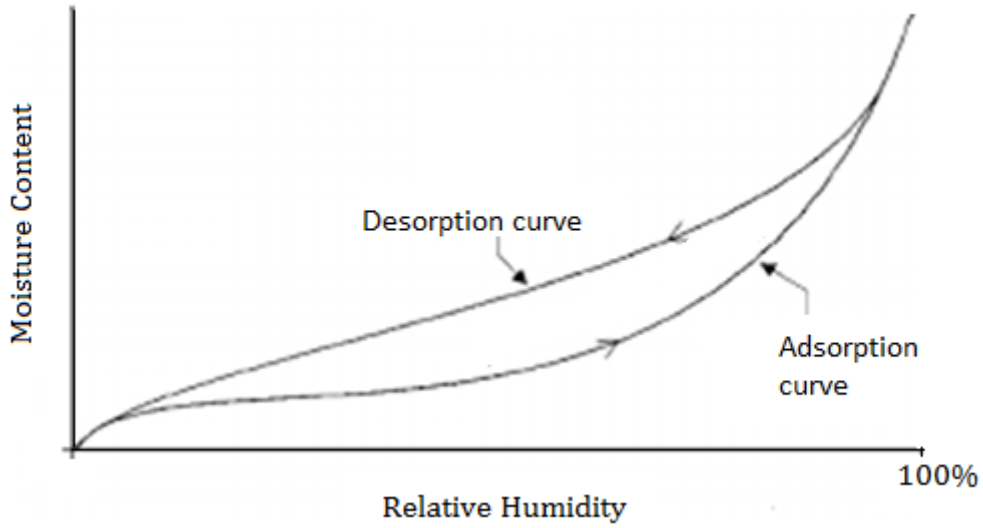

Figure 2.11. The adsorption and desorption curves for sorption of moisture. At extremely high/low RH the difference between the two sorption curves appears non-existent.

The loop effect seen in *Fig. 2.11* is a phenomenon called hysteresis and shows that the amount of water molecules bound to the surface of the fibres and in the fibres pours structure strongly depend on the moisture history of the paper *(Kajanto and Niskanen 1998).* The effect is most prominent in the middle of the curves and the smallest differences in the moisture content is achieved at very high or very low levels of moisture.

A common mathematical model to calculate the moisture content in correlation to the hysteresis curves is the GAB- model presented in *Eq. 8.*

$$Moisture\ content = \frac{m_o(C \cdot k \cdot A_w)}{(1-k \cdot A_w)(1-k \cdot A_w + C \cdot k \cdot A_w)} \qquad [8]$$

Where M_o is the moisture content of the monolayer of water layered on the internal surface of the paper, C is the Guggenheim constant; A_w is the activity of the water and k is a factor depending on the properties of the multilayer molecules with respect to the bulk liquid adsorbed. At a low relative humidity, the water molecules is adsorbed to form a monolayer on the surface of the fibres. An increase of the relative humidity increase the water activity which results in more vapour being adsorbed to the fibres on top of the monolayer film. As A_w increase it will cause changes in the bulk properties, hence changes in k, causing a more rapid adsorption of the water vapour. *(Rhim 2010).*

Due to the different sorption processes a sample can hold different levels of moisture content depending if the sample was pre-conditioned at high respectively low RH. Because both tensile and compression properties are affected by the moisture content in the paper it is important to precondition the materials at lower RH than 30% to attain reproducible equilibrium moisture content *(Frank 2014, Markström 1999, Benson 1971, Fellers and Bränge 1985).*

When corrugated boxes are loaded over time periods, they will deform due to creep. Creep is affected both by the load, time and the humidity. The presence of higher levels of humidity results in a speed up rate for the deformation of the box and it is therefore important that the materials used for corrugated boxes are able to withstand the influence of moisture. Higher levels of moisture will shorten the lifetime of the corrugated boxes. Cyclic conditions at different RH also accelerate the creep in the boxes *(Frank 2014, Back et al. 1983).*

Cellulose and hemicellulose are hydrophilic molecules that will absorb and hold water molecules from the surroundings. Sorption of water vapour causes changes in the structure of the paper on a molecular level by replacing hydrogen bonds, both intra- and inter bonds in the cell wall structure. Presence of water causes the fibres to swell, mainly increasing the width of the fibres and resulting in a lowering of the density of the sheet. Moisture in between the fibre-fibre bonds lowers the effective bonded area between the fibres, resulting in a decrease in stiffness and strength in the paper *(Back et al. 1983, Chalmers 1999, Navaranjan et al. 2012).*

Chalmers (1999) presented a study on how high levels of humidity changes the Young's modulus of the tensile and compression stress-strain curve for linerboard and recycled based medium. His result showed that the elastic modulus decreased at higher RH, and that the Young's modulus was reduced to a greater degree in tension, which disagrees with earlier statement that the compressive stiffness and tensile stiffness are the same, see section 2.3.2. For low levels of RH the difference between the Young's modulus in compression resembles that in tension *(Chalmers 1999).* Virgin fibres have also been reported to loose less of the elastic modulus and strength in compression compared to recycled fibres *(Navaranjan et al. 2012).* The subject of how much the stiffness differs between compressions and tension is sparsely studied and so is the reason why humidity affects the two parameters differently.

3. Experimental

3.1. Material

All materials in this study can be seen in Fig 3.1. The virgin based paper is produced at Gruvön mill, while the recycled based paper was produced by a third party. The grammage of the different virgin qualities was chosen to investigate if humidity affects high weight paper differently than low weight paper. The grammage of the recycled qualities was chosen to resemble the virgin qualities, to be able to compare the results between the qualities and study the differences between virgin and recycled materials. The grammages was sampled to investigate if the moisture affected thin paper differently than thicker paper.

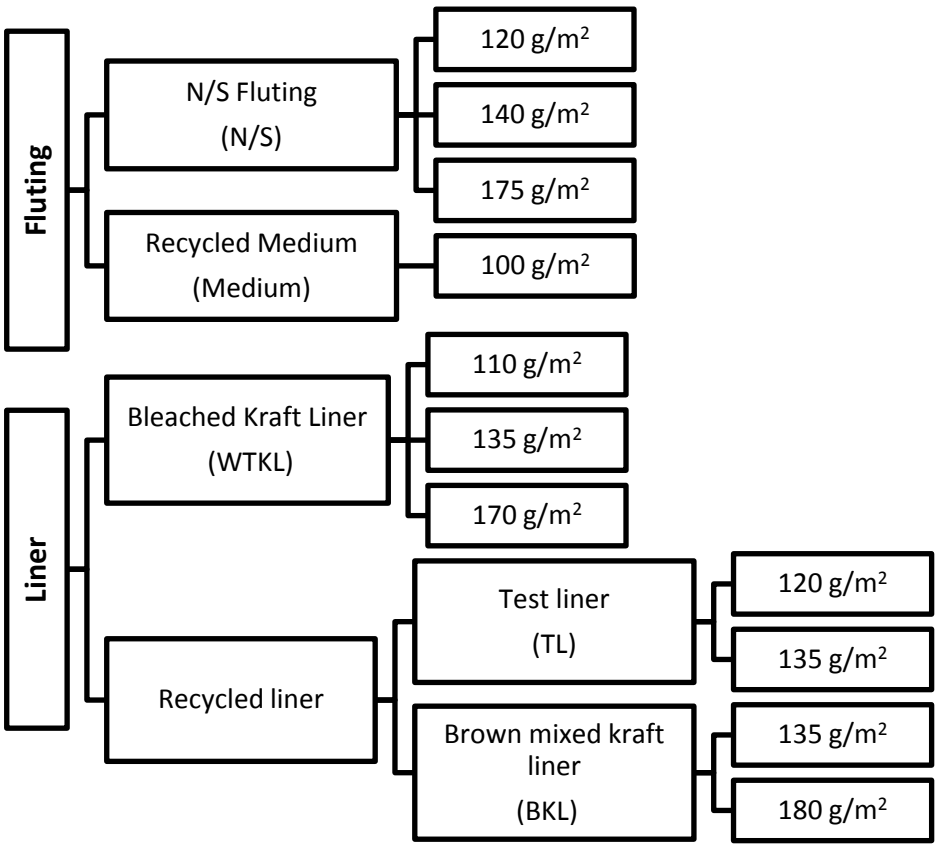

Figure 3.1. Schematic view on all materials and different grammages (g/m^2) used in the study.

The letter combination presented inside the brackets in *Fig. 3.1* will be used throughout the report. Table 3.1 present the shapes of the fibres found in the different qualities.

Table 3.1. Data describing the appearance of the fibres in the different materials.

	Mean length [mm]	Mean width [µm]	Mean shape [%]
WTKL	1.351 ± 0.041	24.3 ± 0.3	89.7 ± 0.1
BKL	1.387 ± 0.007	29.0 ± 0.4	89.8 ± 0.1
TL	1.204 ± 0.028	27.7 ± 0.0	90.2 ± 0.3
N/S	1.042 ± 0.013	28.4 ± 0.0	93.5 ± 0.4
Medium	1.154 ± 0.016	28.2 ± 0.4	89.6 ± 0.0

The mean shape of the fibres describes how much kinks/ curls the fibres have. A straight fibre has a high value of the mean shape.

3.1.1. Conditioning of samples at 50% RH

At 50% RH the samples were prepared by the same method as used by the analytical laboratory in the everyday testing of both liner and fluting. Sheets which came freshly from the production were pre-conditioned in a climate less than 30% RH for a minimum of 48 h to make sure the hysteresis effect of the sorption of moisture followed the primary adsorption curve.

Paper sheets were placed over a grid which has a vacuum effect on the backside for 10 minutes. The vacuum sucks moist air (50% RH) through the fibre network, thereby speeding up the adsorption of water vapour onto the fibres in the paper. The standard conditions in the paper analytical lab follow ISO 187:1990.

3.1.2. Conditioning and preparation of samples at 90% RH

All samples conditioned at 90% RH were prepared at 50% RH to minimize the loss of moisture in each sample before testing the mechanical properties. After preparation the samples were placed in a climate chamber which holds a temperature of 20°C and a RH of 90% for at least 48 hours.

Fresh sheets were pre-conditioned in the same way as new sheets in 50%, but were not conditioned on a grid. This because the hysteresis curve for adsorption and the curve for desorption lies very close to each other at high levels of humidity as seen in the theory.

3.2. Laboratory study

A summary view over the laboratory study can be found in *Fig. 3.2.* All materials used in this study were tested according to this flow chart.

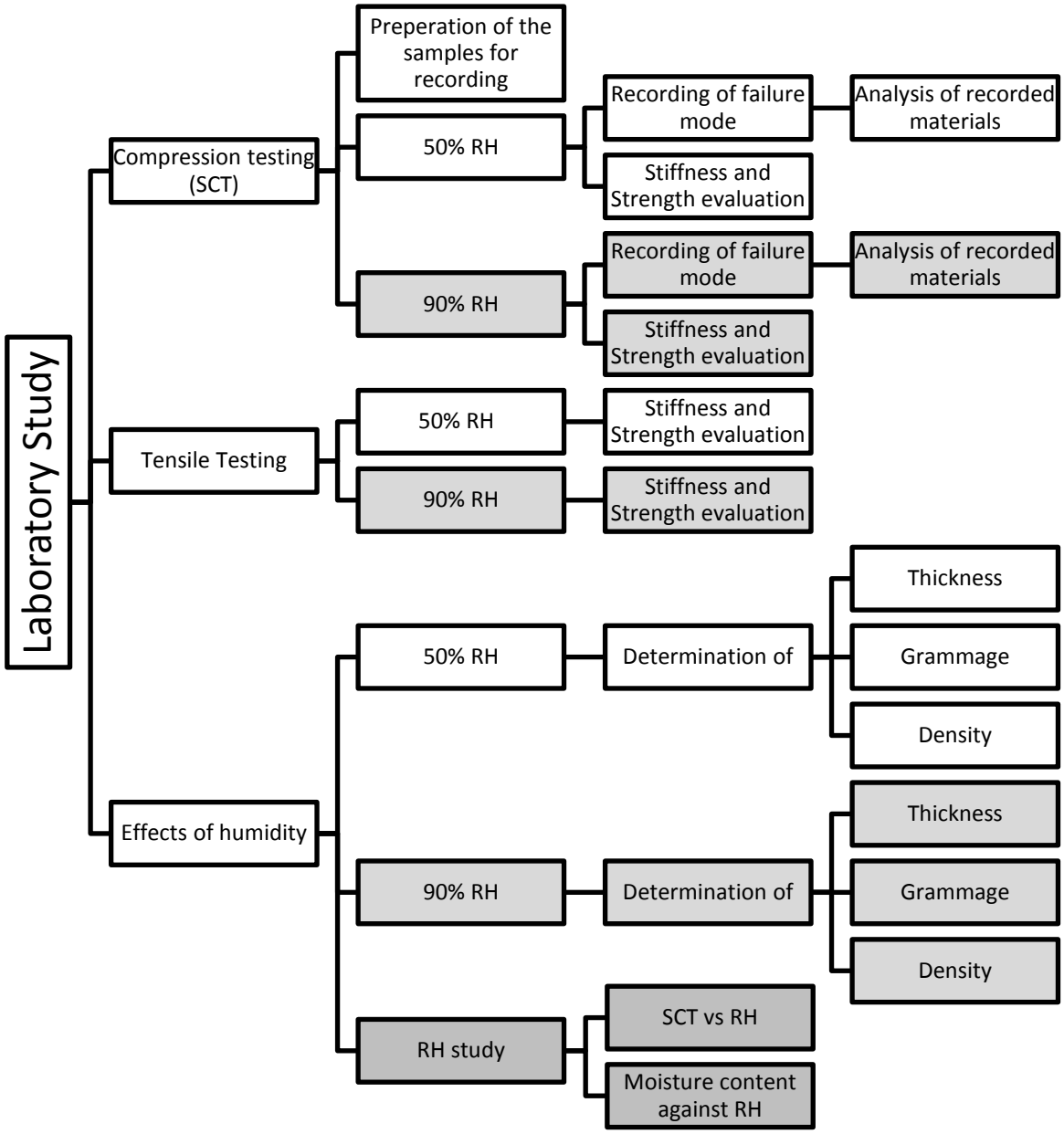

Figure 3.2. Overview of the procedure for the laboratory study used for all materials. Conditioning of samples at higher relative humidity is marked with the coloured boxes.

For the recycled medium no concrete trend can be seen due to the study only had access to one grammage.

3.2.1. Grammage, thickness and density

Determination of the grammage and density of the provided materials were performed according to ISO 536:2012 and ISO 534:2011. For evaluation of the thickness of all paper grades, a thickness meter provided by L&W Micrometer was used. For the grammage of the paper, 20 pieces of 1 dm^2 each was

punched out from the paper and weighed in at a laboratory scale with 3 decimals precision. The measured grammage was used in the calculations of the indexed strength and stiffness values.

3.2.2. Anisotropy

The Anisotropy of the different materials was calculated according to *Eq. 9* using the tensile stiffness at 50% RH. The anisotropy of the different papers can be seen in *table 3.2.*

$$A_E = \frac{E^b_{T.MD}}{E^b_{T.CD}} \qquad [9]$$

Table 3.2. Anisotropy in the paper.

	Grammage	Anisotropy
WTKL	110	2.5
	135	2.4
	170	2.3
BKL	135	2.5
	180	2.3
TL	120	1.7
	135	2.1
NS	120	2.5
	140	2.4
	175	2.3
Medium	100	2.4

3.2.3. Tensile properties

The tensile properties were evaluated in a Zwick /Roell AllroundLine. Paper samples were prepared in both MD and CD according to ISO 1924-3:2011. In normal testing of tensile stress and strength, the Zwick has a pre-load of 5 N to remove the "slack" part of the curve to make the determination of the stiffness easier. A drawback of the preload is that everything that happens below 5 N will not be recorded by the software. In 90% RH this could result in a different stiffness value as the sheet network may already has begun to deform plastically below the 5 N preload, due to the increased moisture content. Therefore, the preload was removed before measurements at 90% RH were conducted to make sure all data was included.

Samples tested in 90% RH were carried out on a Zwick placed within BillerudKorsnäs climate chamber that holds a constant climate of 20±2°C and 90±1% RH.

Each tensile curve was evaluated in the Zwick software program TestXpertII for tensile strength and tensile stiffness. In addition, a 95% confidence interval was calculated for all test series.

3.2.4. Compression properties

The compressive strength was evaluated for all paper grades with an L&W STFI compressive strength tester according to ISO 9895:2009. A 95% confidence interval was then calculated for each sample series.

For measurements of the SCT value of paper conditioned at 90% RH the samples where tightly packed in a plastic bag and placed in an envelope, which had isolating bubble wrap on the inside. This was

done to prevent moisture content loss in the paper, as the SCT machine was located in a different lab than the climate chamber.

From the SCT machine, the distance between the clamps and the force applied on the test sample were acquired and was used to plot a force-displacement curve, from which the compression stiffness was evaluated. When studying the deformation from the clamps displacements, it became apparent that these values did not correspond to the deformation in the paper due to sliding. The calculated strain value was of the order 5-10%, while the literature described strain one magnitude lower. (*Gunderson et al. 1988, Chalmers 1998 and Fellers and Gimåker 2011*, *Borgqvist 2016*). This presented a problem when plotting a SCT curves against a tensile curve due to that the elongation/compression of the paper was not representing the same thing. This will be further discussed in section 4.2.4.

For the compression properties in the relative humidity study the papers are only tested in the CD direction, due to that being the load bearing direction for the medium in the finished containerboard.

3.2.5. Visual recording of SCT test

All SCT measurements were recorded at 30 fps with an iPhone 6 equipped with a ōlloclip 15x Macro lens. The camera was placed over the gap between the SCT machine's clamps. All recordings were at the resolution 1920x1080 px. Snapshots taken from the recordings hold a resolution of 1334x750 px, which is equal a scale of 496 px/mm.

To get an optimal view of the fibre network and the failure modes during the recording, all test pieces had one side of the sample cut using a utility knife. The cut side was marked to make sure it was orientated against the camera during recording. This method of cutting was reproduced from Hansson's study (2013), in which he studied different ways to prepare a SCT test piece for optimal view of the cut surface for microscopic recordings.

The recorded material was used to determine different failure modes in the structure, to see if a certain type of failure correlated to type of paper and if one type of failure mode correlates to the strength and stiffness of the materials. The failure modes were described by Hansson (2013).

3.2.6. STFI Short span compression tester.

Recordings of the compression tests showed that the paper samples slide between the clamps. As mentioned in section 3.2.4., it is the distance between the clamps that is evaluated by the SCT test. This results in that the actual compression of the paper itself remains unknown.

To get the actual compression of the paper, a series of recordings where performed on N/S and WTKL grades, in both MD and CD. Each strip was marked with lines that held a distance of 1 mm in between. Each recording was then studied and snapshots were taken at the moment of "clamping" on the sample and at the moment before failure. Each photo was then evaluated by measuring the change in distance between the lines between the starting position and the moment of failure. The change in the distance between the start position and the moment of failure could then be interpreted as the actual compression of the paper piece. See *Fig. 3.3*.

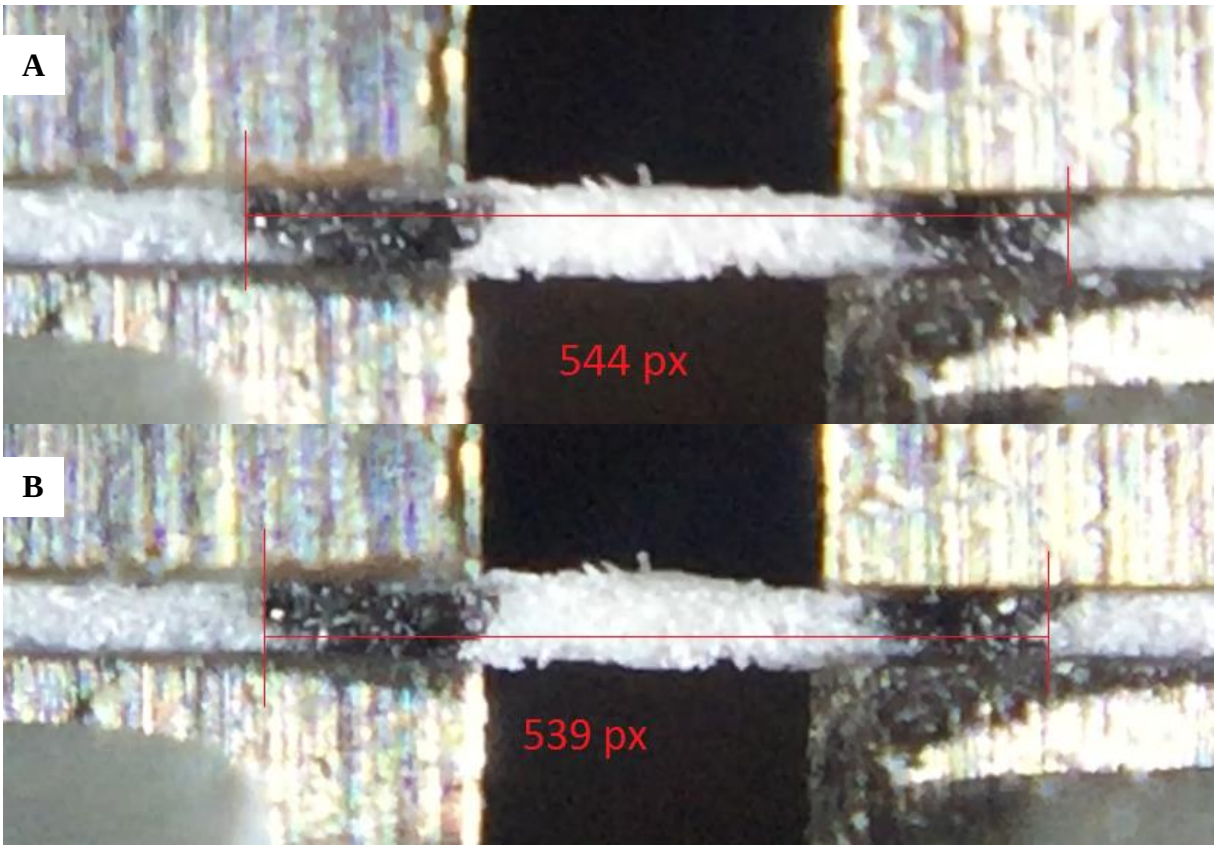

Figure 3.3 Compression of the paper during the SCT measurements. A. show the starting position and B the moment before failure. 1 mm = 496 px.

From analyses of the recordings the actual compression of the paper was approximated to be 0.1-0.15% for every 1% change in the distance between the clamps. This approximation however was calculated with a big uncertainty which resulted in the method was deemed to untrustworthy for continual usage. Borgqvist (2016) experienced the same problem when he simulated the compressive behaviour in SCT testing of paperboard.

To be able to calculate the actual strain of the paper in compression that correspond to the reported strain values from literature by Gunderson et al. (1988), Chalmers (1998) and Fellers and Gimåker (2011), the assumption that the stiffnesses are the same in tensile and compression was used, as discussed in section 2.3.2. A factor α_{SCT} was calculated by taking the quotient between the measured E-modulus for compression and tensile conditioned at 50% RH, see *Eq 10.*

$$\alpha_{SCT} = \frac{E_C^{50}}{E_E^{50}} \qquad [10]$$

By using α_{SCT} to rescale the strain data from the *SCT* test for paper conditioned at both 50% and 90% RH. The stiffness for *SCT* samples conditioned at 90% RH was also re-evaluated with α_{SCT} to be able to compare the results with the tensile stress strain curve, see *Eq 11*.

$$E_C^{90} = \frac{E_{SCT}^{90}}{\alpha_{SCT}} \qquad [11]$$

A complete list of the calculated values of α_{SCT} for the different materials can be found in *table A.1* found in Appendix I.

The rescaled curve showed similar stress-strain relations as the literature described. However, whether it is correct to use *Eq 10* and *11* to calculate the value of the compression stiffness at 90% RH from the compression and tensile stiffness at 50% RH can be argued against, but is used in this study to evaluate if there is a difference in the stiffness at 90% RH between compression and tension.

To determine if sliding between the clamps could be related to the friction of the paper, the friction angle was determined for all materials. The friction angle was determined by clamping one larger piece of paper to a plate with the ability to change and measure the angle. The test piece was orientated with the MD direction in line with the intended sliding path. A sledge was mounted to a second piece of paper, cut to 40x40 mm, from the same quality. The sledge was placed with the sledge samples MD direction 90° against the intended sliding path. A sensor located above the surface of the clamped test piece was activated when the sledge was placed against it and started to increase the angle of the plate. As the sample started to slide, the connection between the sledge and the sensor was severing the contact between the sledge and sensor. The friction angle could be registered from how high the end of the plate had risen. The procedure was carried out five times for each quality. A low friction angle implies that the paper have a low friction constant.

3.3. Determination of moisture content in paper

Several authors state that humidity affects the mechanical properties of fibrous materials negatively *(Chalmers 1998, Page 1969, Back et al. 1983, Fellers and Bränge 1985).* It was therefore crucial to evaluate how the SCT value varied with varying levels of RH to investigate if the mechanism for moisture adsorption at different RH corresponds to changes in SCT.

To achieve desired RH for conditioning, a method of using saturated salt solutions in a closed environment was used. The relation between certain salts solutions and a corresponding RH is well known and the type of salt chosen for the pre-study will correspond to RH between 33-95%. The RH achieved from a salt solution is known to be accurate and was used in laboratories before modern conditioning technologies was available and have therefore been extensively studied. *(Greenspan 1976).* The salts in *Table 3.1* were therefore chosen according to existing tables presented by Greenspan (1976) and Rockland (1960)

Table 3.1. Salts used for the pre-study. The reference RH was conditioned in a laboratory with standard conditions.

Salt	**Desired RH**
Dry	0%
Magnesium Chloride	33%
*Reference	50%
Sodium chloride (NaCl)	75%
Ammonium chloride ($(NH_3)_2SO_4$)	80%
Potassium chloride (KCl)	85%
Barium dichloride ($BaCl_2$)	90%
Potassium Nitrate (KNO_3)	95%

100 ml saturated solutions of each kind of salt were prepared and placed in an airtight container and left to stand in a conditioned laboratory, which held a constant temperature of 23°C. To verify the RH within the container a polymer based capacitive RH sensor with an accuracy of ±3% was used. The instrument was not suitable for accurate measuring above 95% RH.

Paper samples were cut out to 1 dm^2 and then dried at 105°C for 15 minutes to remove all moisture. The samples were then marked and weighed before being placed above the salt solution inside the container and left for conditioning for 48h.

After the samples were conditioned the moisture content in the paper could be determined with *Eq. 12* after a second weigh-in.

$$MC = \frac{m_{RH} - m_{Dry}}{m_{Dry}} \cdot 100 \qquad [12]$$

Where m_{RH} is the weight for the conditioned samples, m_{Dry} is the samples dry weight and MC is the moisture content in % in the paper.

10 SCT samples in MD from the different qualities were conditioned at different RH for 48 h to investigate how the moisture content within the paper affected the compression strength of the paper. The samples were prepared according to ISO 9895:2009. When transporting the SCT samples, the same procedure was used as for the conditioning at 90% RH. The result from the SCT measurements was plotted against the moisture content in the paper.

4. Results and discussion

In this study the strength and stiffness of liner and fluting at 50% RH and 90% RH have been evaluated. The following sections present and discuss the results achieved and compare the different mechanics behind the failures of the paper in compression and tension.

4.1. Stiffness and strength retention at 90%RH

In following sections the results of the stiffness and strength measurements presented. The results are presented as the retention of the stiffness/strength at 90% RH compared to the original value at 50% RH, calculated by *Eq. 13*. All figures include the retention for both tension and compression stiffness/strength.

$$\mathrm{Re}\,tention = \frac{X_{90}}{X_{50}} \cdot 100 \qquad [13]$$

Where X_{90} is the strength or stiffness property at 90% RH and X_{50} at 50% RH.

4.1.1. Linerboard

Fig. 4.1 and *4.2* show the results of the tensile stiffness and compression retention at 90% RH for linerboard.

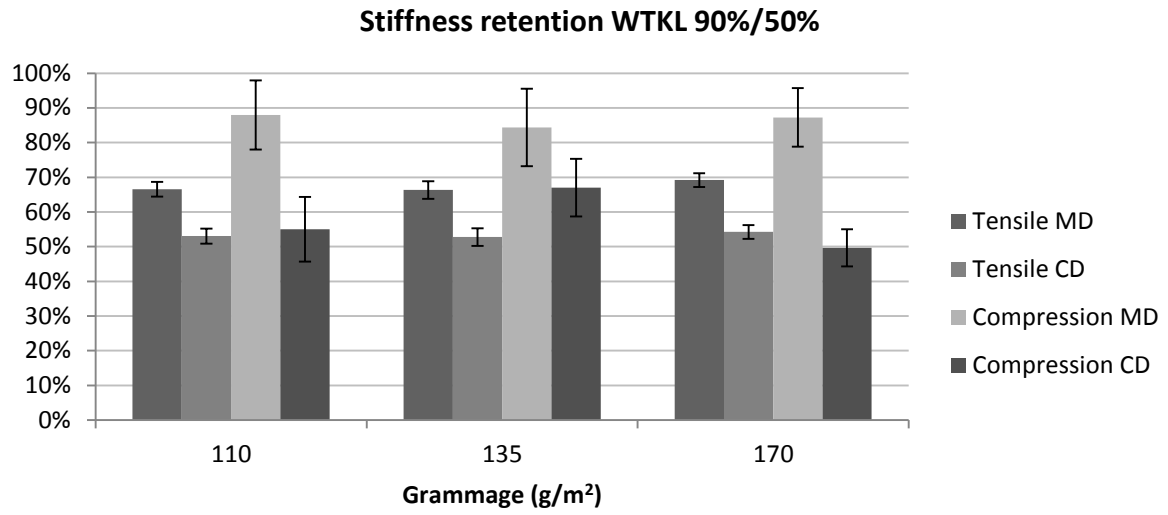

Figure 4.1. Stiffness retention at 90% RH for WTKL.

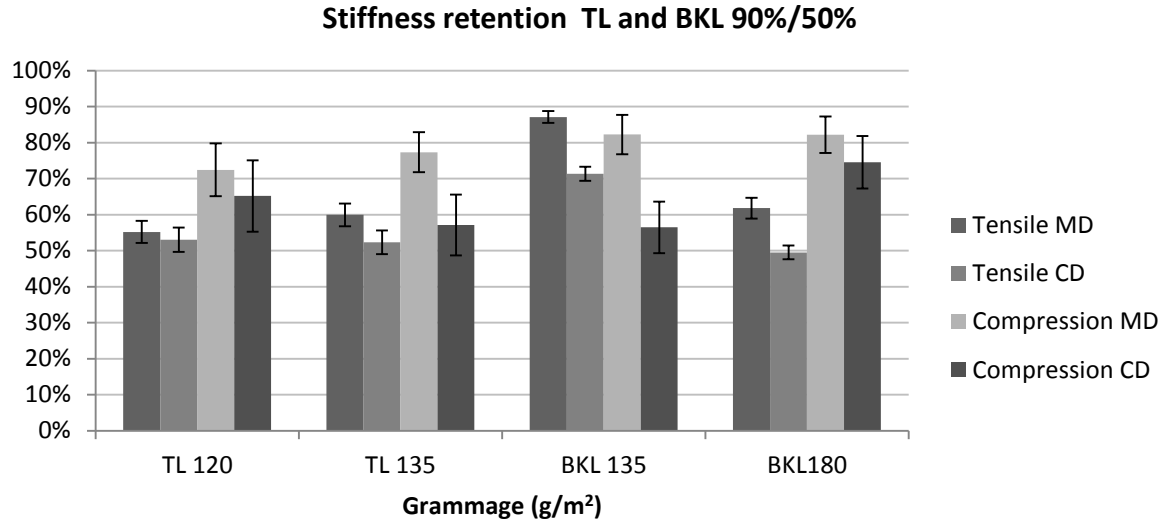

Figure 4.2. Stiffness retention at 90%RH for recycled linerboard.

As the result shown in *Fig. 4.1* and *4.2*, virgin fibres retain between 65-70% of the original tensile stiffness in MD compared to the recycled fibres which retain 50-60%. In CD the differences between virgin based materials and recycled materials smaller as all qualities retain between 50-55% of the tensile stiffness. The retention of the stiffness also appears to be independent of the grammage. One exception is found, BKL 135, which appears to retain significantly higher values of its tensile stiffness in both MD and CD.

When comparing the different directions of the paper all but TL120 retain more of the tensile stiffness in MD than CD. This can be because of the anisotropy of the paper. The anisotropy of the TL120 where approximately 1.4 whiles the remaining linerboards had anisotropy values above 1.8. It would be interesting to produce laboratory sheets with different anisotropy to study if the retention of the strength and stiffness properties are correlated to the anisotropy of the fibre network.

All linerboard materials appear to retain large parts of the original stiffness in compression at 90% RH. Virgin fibres tend to retain more than the recycled materials but due to the distribution of the measurements no final conclusion can be made. The retention of the compression stiffness in CD lies around 55-60% with the exception of BKL180.

The retention of both strength and stiffness was evaluated from compression and tensile measurements by calculating the stiffness (or strength) value at 90% RH divided with the stiffness value at 50%RH. What *fig 4.1 and 4.2* illustrate is just the difference between the two different conditions. Even if it appears like there are small differences in how much stiffness the paper loses at high RH the absolute stiffness for virgin fibres exceeds the stiffness for recycled fibres. Se *Fig 4.3 – 4.4* for comparison between the different qualities. All data have been normalized against the grammage to be able to compare the materials between different grammages and qualities.

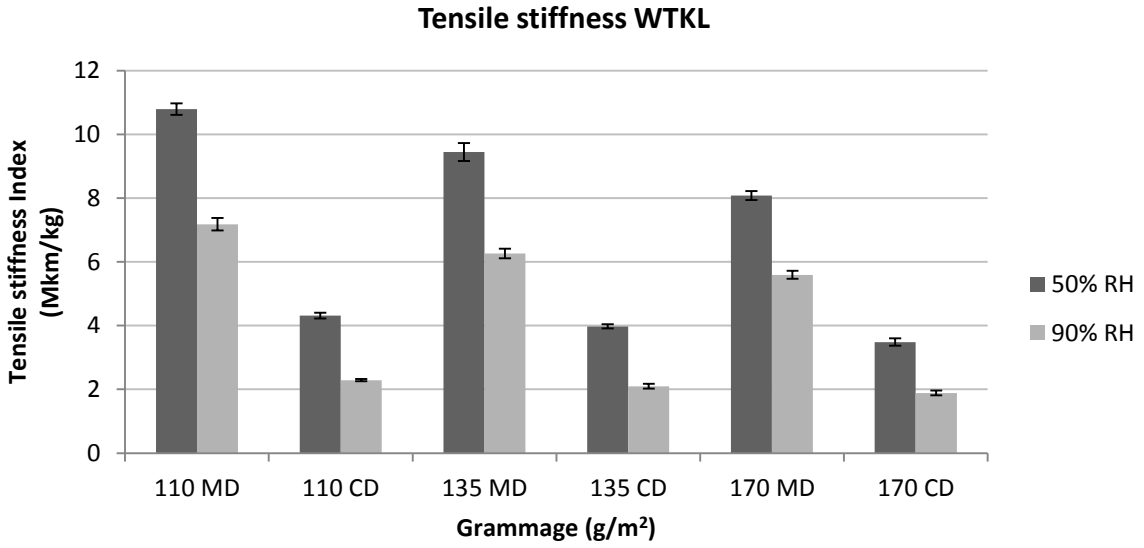

Figure 4.3. Absolute stiffness of the WTKL in 50%RH and 90%RH

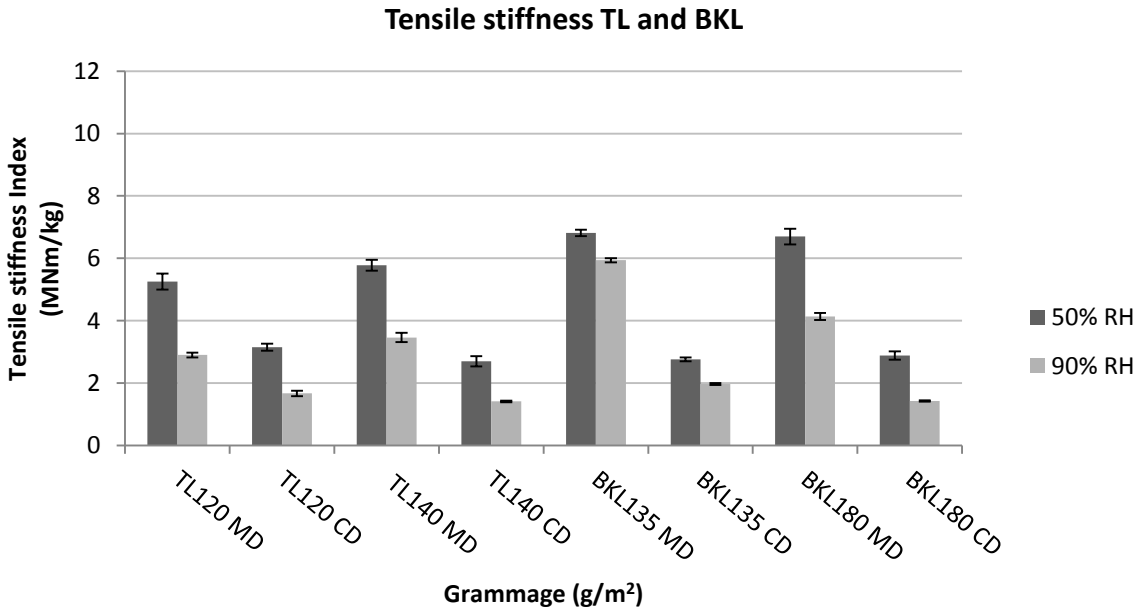

Figure 4.4. Absolute stiffness of the recycled materials in 50%RH and 90%RH

Fig 4.3 -4.4 shows clearly that virgin fibre based liner is stiffer than liner based from recycled fibres, both initially and when conditioned at 90% RH. These results agree with results found in the literature. (*Zhang et al. 2001, Lindström 1986)*. The same trend that can be seen for the tensile stiffness can be seen for the compression stiffness and both tensile strength and stiffness. In *Fig 4.3.* the stiffness index WTKL 120 is higher compared to the heavier grammages and can be due to the production of WTKL 120 is done on a different machines compared to the other two grammages. Figures over the absolute stiffness and strength for the remaining materials are displayed by *Fig A.1-A.14* located in Appendix II.

Fig.4.5 and *4.6* represent the strength retention for the different linerboards.

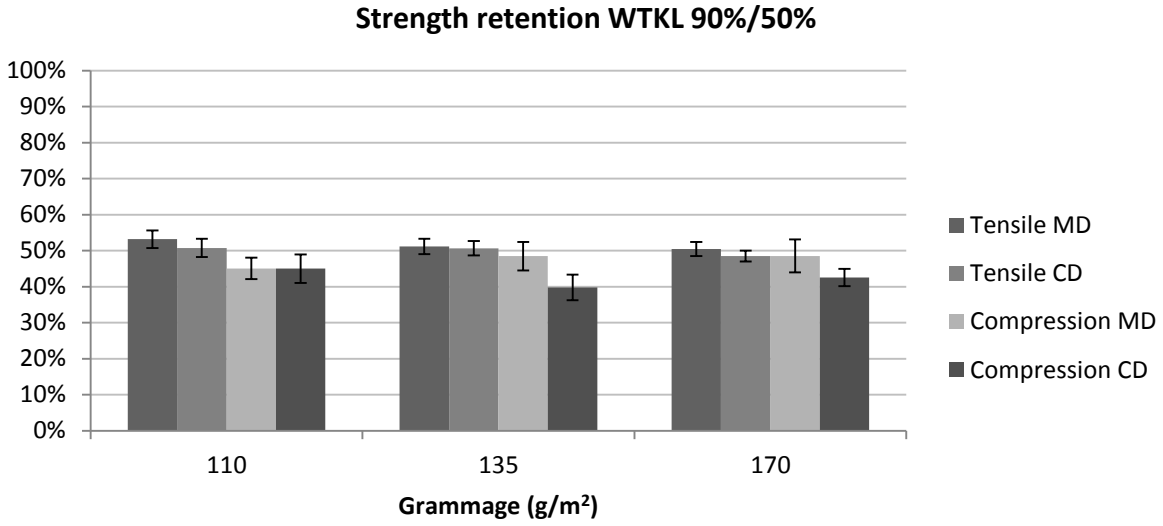

Figure 4.5. Strength retention in WTKL at 90% RH.

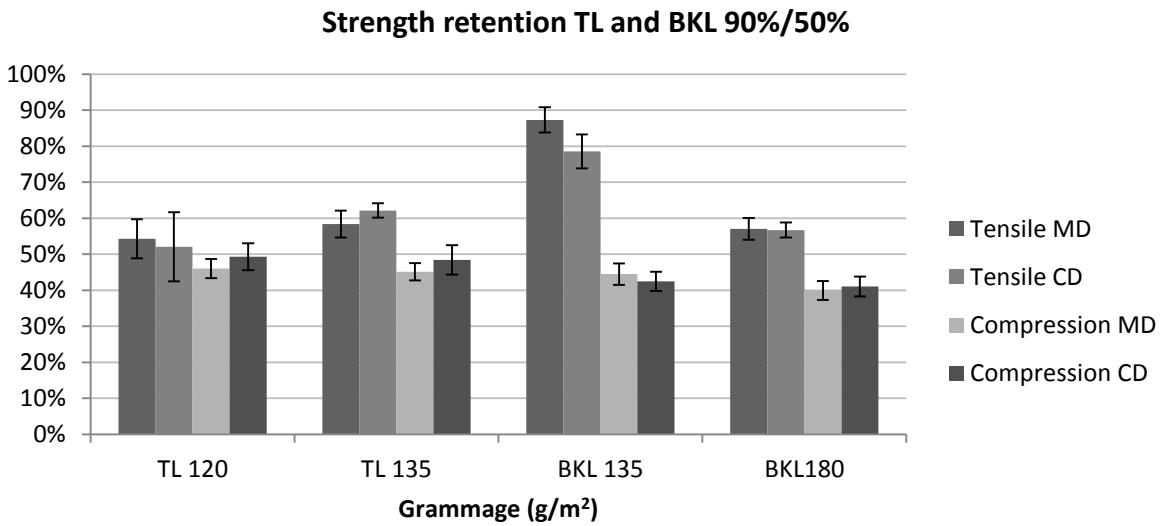

Figure 4.6. Strength retention for recycled linerboards at 90/% RH.

When comparing the retention of the strength of the different linerboards, recycled linerboard appears to retain more of the original tensile stiffness than virgin fibres, and significantly more in tensile than in compression. However, as discussed in the previous section the graphs are not to be confused with the actual strength of the paper. When comparing the retention of the compression strength, all materials seem to retain equal amounts of their original compression strength.

BKL135 show the same significant difference from the other materials in the strength retention as the material displayed in the stiffness retention results.

As discussed by Zhang et al. (2001), Navarajan et al. (2013) and Retulainen et al. (1998), recycled fibres have a reduced ability to absorb water due to hornification. The stiffer recycled fibres make out a stiffer network that does not experience the same plastic deformations as the one a virgin fibre network experiences. With the addition of the fact that the recycled fibres have a reduced capacity to form fibre-fibre bonds the performance of the paper results in lower yield points for the elastic

deformation and an overall lower strength in the paper. But the results also give the appearance of higher ability to retain the strength and stiffness.

4.1.2. Fluting

Fig. 4.7 – 4.8 show the stiffness retention for the different fluting materials

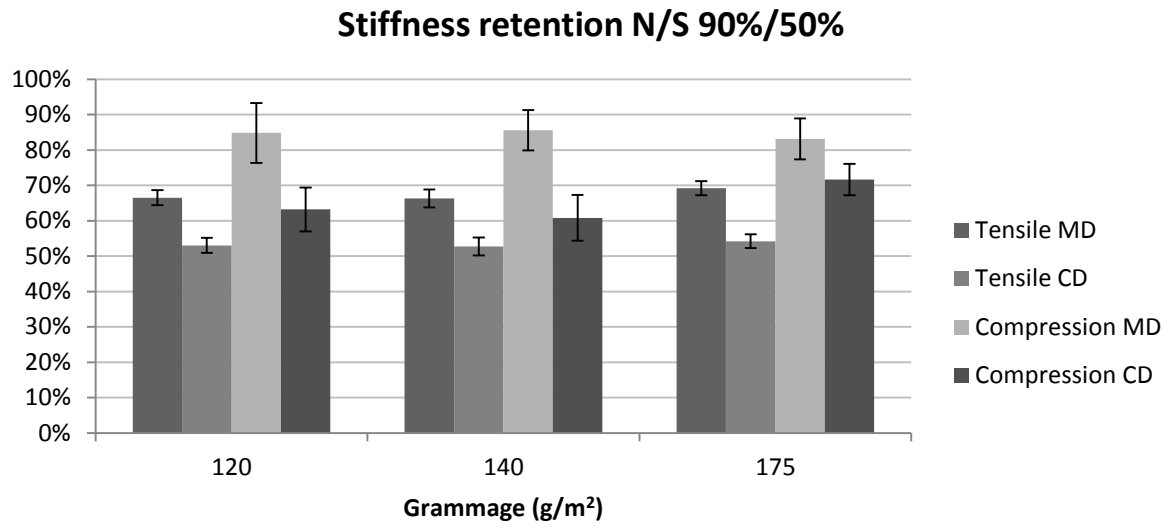

Figure 4.7. Stiffness retention in N/S fluting.

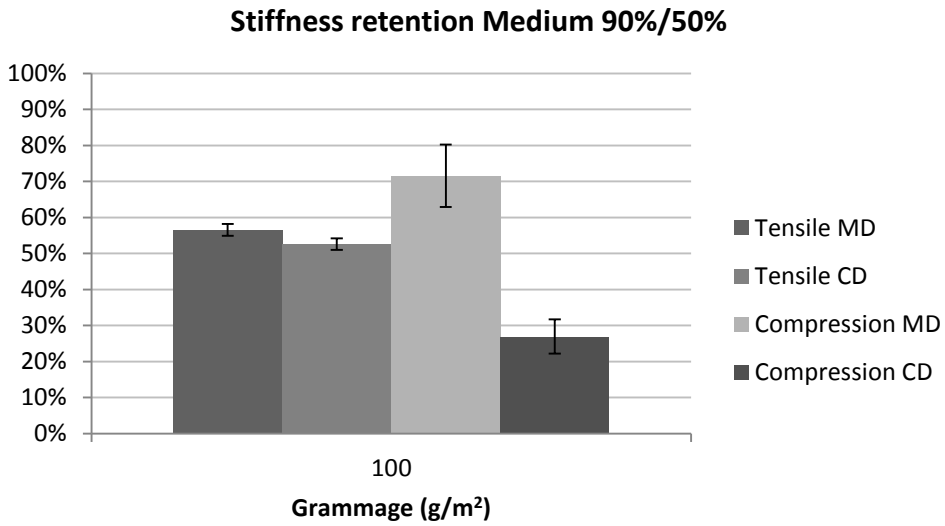

Figure 4.8. Stiffness retention of recycled medium.

When comparing the N/S fluting to the recycled medium the results show that the virgin fluting retain above 65% of the original stiffness in tension and above 85% in compression. The results are similar to those of the linerboards in that the retention of the stiffness in compression is higher than for tension and that it is a significant difference between MD and CD (for the virgin based paper).

When studying the stiffness retention of the recycled medium, the compression stiffness in CD is significantly lower than that of the N/S medium. The difference in retention between the MD stiffness and CD stiffness in tension is small, though MD appears to retain more. Unlike TL 120, the small

difference between MD and CD is not because of the anisotropy of the paper as it was similar to the N/S qualities anisotropy.

The differences in the compression stiffness retention can be explained by the starch present in the recycled paper. Starch is added in paper to improve the fibres ability to form fibre-fibre bonds and consequently improve the dry strength of the material. Compared to cellulose, starch is a highly hydrophilic compound which is solvable in water. The structure of starch is that of a large polysaccharide chain that is connected by α-glycosidic bonds which results in an amorphous structure *(Richardson and Gorton. 2003).* At higher RH, starch adsorbs high amounts of moisture and would therefore also be affected by the moisture in the same way as cellulose and hemicellulose. For a paper network it will result in losses of the supportive function to the recycled fibres strength and stiffness abilities.

Fig 4.9 and *4.10* shows the strength retention for the fluting materials.

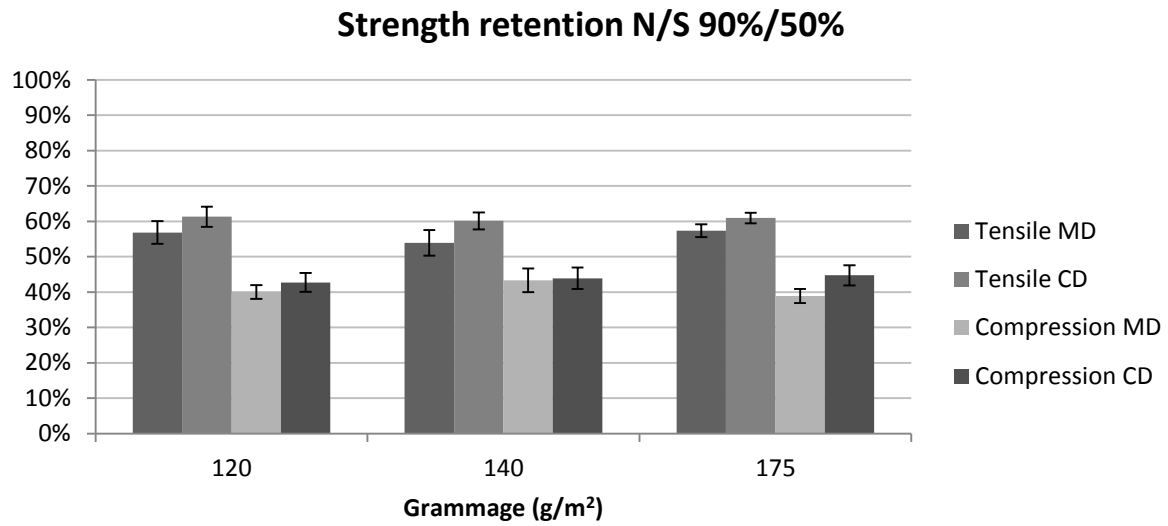

Figure 4.9. Strength retention for N/S fluting.

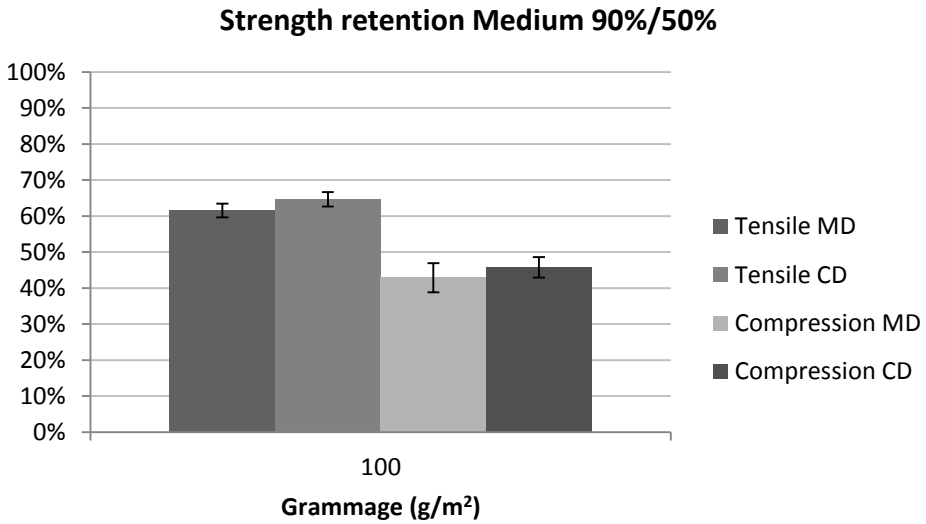

Figure 4.10. Strength retention for recycled medium.

The strength retention for the fluting materials appears to be about the same for virgin fibres and recycled fibres. As Fig *4.3* and *4.4* showed for the linerboards it is important to keep in mind that the retention of the strength and stiffness does not give any indication of the actual strength or stiffness of the paper. By just comparing the recycled medium to the N/S fluting, it would be easy to say that it would not matter which material was used in corrugated boxes. But when considering the total strength and stiffness the virgin N/S fluting far surpass the recycled based medium. Se *Fig. A-II.1* to *A-II.14* in appendix II.

To summarise the result presented in this study under section 4.1.1 and 4.1.2 the result show that virgin based paper retain about the same amount of their original stiffness and strength when expesed to high levels of humidity. It is therefore important to remember that the absolute strength and stiffness of virgin based materials exceeds the corresponding values in recycled products as they are more likely to be able to survive longer periods of time in high RH climates.

4.1.3. Influence of humidity on the stiffness in paper.

As the result represented in *Fig. 4.1-4.2* and *4.7-4.8* the retention of the stiffness properties differ significantly between tensile and compression at 90% RH. The difference in the stiffness between compression and tension is evaluated by *Eq 14.*

$$\textit{Difference in the compressive and tensile stiffnesses} = \frac{E_C^{90}}{E_T^{90}} \cdot 100\,[\%] \qquad [14]$$

In *Table 4.1-4.4* the difference in the stiffness between the two properties are found. In the tables show the absolute confidence interval calculated with 95%

Table 4.1. The difference in compression and tensile stiffness at 90% RH for WTKL

WTKL	MD	±	CD	±
110	131.3%	13.6%	112.2%	11.4%
135	106.6%	8.5%	115.5%	11.0%
170	103.0%	8.2%	139.2%	11.0%

Table 4.2. The difference in compression stiffness and tensile stiffness at 90% RH for recycled linerboard.

Recycled Linerboard	MD	±	CD	±
TL 120	131.3%	12.5%	122.9%	17.6%
TL 135	129.1%	10.3%	109.2%	10.5%
BKL135	94.4%	4.3%	79.1%	7.3%
BKL180	133.0%	7.2%	50.6%	4.2%

Table 4.3. The difference in compression stiffness and tensile stiffness at 90% RH for N/S.

N/S	MD	±	CD	±
120	127.5%	12.1%	119.2%	10.0%
140	129.0%	7.4%	115.3%	9.5%
175	120.1%	7.4%	132.1%	7.9%

Table 4.4. The difference in compression stiffness of the tensile stiffness at 90% RH for recycled medium.

Recycled medium	MD	±	CD	±
100	126.5%	12.2%	89.1%	14.3%

With the exception for BKL135 MD and CD, BKL 180 CD and medium 100 CD, the results from this study indicate that paper retains more of the original stiffness in compression than the material do in tension, at least for the virgin based qualities. The results for the virgin based papers are consistent with results presented by Chalmers (1998) about the difference between the compression stiffness and tensile stiffness at 90% RH, but when comparing the recycled qualities the stiffness show mixed results.

The decrease of the stiffness in the recycled materials could be because of the starch present in the network. As discussed in section 4.1.2, the starch adsorbs water molecules and the paper loses the support the starch gave. The literature covering the subject of the relative humidity's effect on the starch influence on the strength and stiffness properties in paperboard is sparse. Further evaluation of the subject is needed to be able to understand if the strength and stiffness properties of recycled fibres decrease due to starch adsorption of moisture.

4.2. Compression properties

4.2.1. The compression failure mechanism vs. the tensile failure mechanism

When studying the failure mechanisms, the most prominent difference was the length of the free segment (100 mm for tensile tests and 0.7 mm in the SCT), as well as the difference in the strain rate. In compression, the strain rate is approximately 430%/min which is more than 4 times the strain rate in tension (100%/min). The difference in the strain rate will affect the stiffness performance of the fibres. Gundersson et al. (1988) performed a study where different load strain rates were used. The results clearly indicated that the stiffness of the paper depended on the load rate. It would therefore be interesting to study where the strain rate in tension is adjusted to the same strain rate as the SCT machine express and investigate how the results compare to the SCT results.

In tensile it results in that the entire fibre network gradually is put under load. Initially, the network becomes "straighten out" and fibres aligned in the loading direction become activated. As more load is applied, an increasing amount of fibres become activated until the yield point at which the network starts to deform plastically due to shear forces and fibre rupture.

On a fibre network level, the degree of bonding between the fibres contributes to the total strength of the network, effectively relating to the tensile and compression strength and stiffness of the paper. *(Hansson 2013, Shallhorn et al. 2004, Fellers and Gimåker 2011).* During the SCT testing the short span of 0.7 mm is shorter than the average length of a hardwood fibre, which can range between 0.8-1.8 mm. *(Daniel 2009, Sjöström 1981).* It can therefore be assumed that all fibres will span over the free segment and be fixated by the clamps. This scenario is most likely to be observed in MD due to the orientation of the fibres. In CD however, it is possible that less fibres will span the entire free segment and thus experience more shearing forces caused failures. This also explains why the elastic part and the point of failure is much lower for compression compared to tensile testing.

As the SCT test starts, all fibres are activated at once and the strength and stiffness properties of the fibres will therefore affect the results to a larger degree than the shear resistance between the bonding sites (similar to zero tensile strength which is triggered by fibre rupture *(Niskanen and Kärenlampi 1998)*).

The immediate activation of the network can also explain why the compression stiffness differs from tensile stiffness at high moisture content levels as shown in *Table 4.1-4.4*. Due to the swelling in the fibres, the thickness of the walls increases and thus change the relationship for the fibre buckling which counteracts the softening of the fibres in compression. In tension, the softening of the fibres and the fibre-fibre bonds causes a larger decrease of the strength and stiffness due to the shearing forces in the entire network. When critical failure load is reached, the fibre walls start to delaminate and cause a local decrease in the bending stiffness of the fibre, resulting in local buckling and a global delamination in ZD.

As stated by Mäkelä (2010) and observed in this study, the failure mode of the sample can appear as a global buckling failure which does not represent the true compression strength of the board. Further studies of the nature of the compression failures in paper are needed to fully understand and explain why the paper buckles instead of being compressed.

4.2.2. SCT Failure modes at 50% RH and 90% RH

The recorded material was studied and the four different failure modes are identified and named according to the work by Hansson (2013). Examples of the different failure modes can be seen in *Fig. 4.11*.

M1 – Symmetrical failure mode of the paper.
M2 – Asymmetrical failure mode of the paper
M3 – A global bending failure mode of the paper
M4 – No visible failure mode in the paper

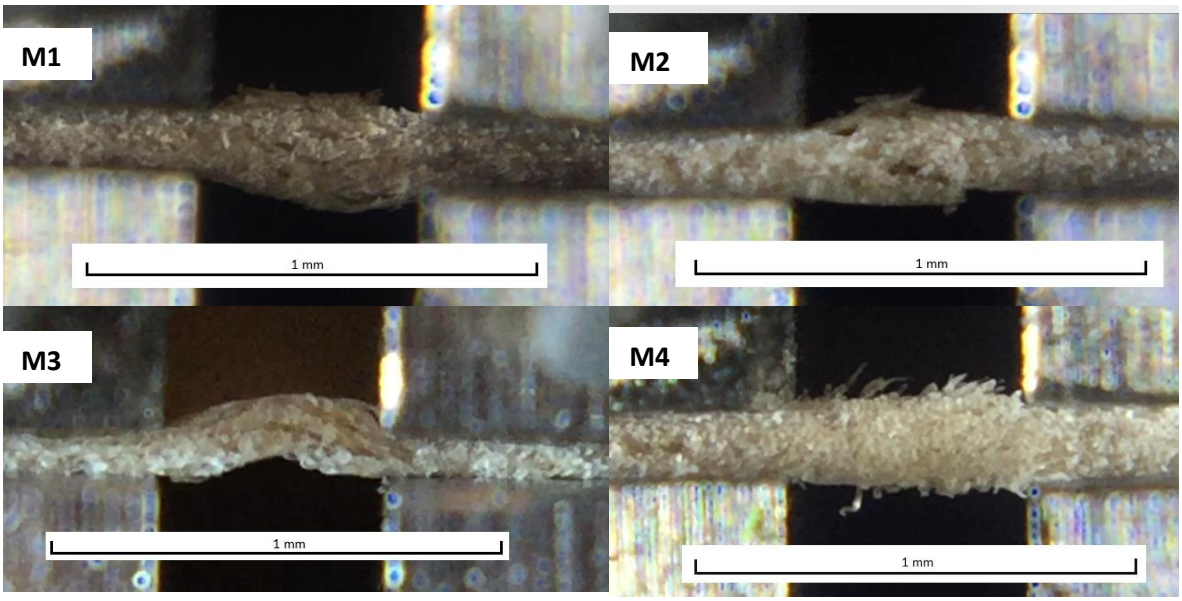

Figure 4.11. Snapshots taken of the four different failure modes seen in the N/S material under compression loads. All modes appeared in the same fashion in the other materials

Fig 4.12-4.14 represents the distribution of compression failure modes for all materials conditioned at both 50% and 90%. Each column represent 10 samples.

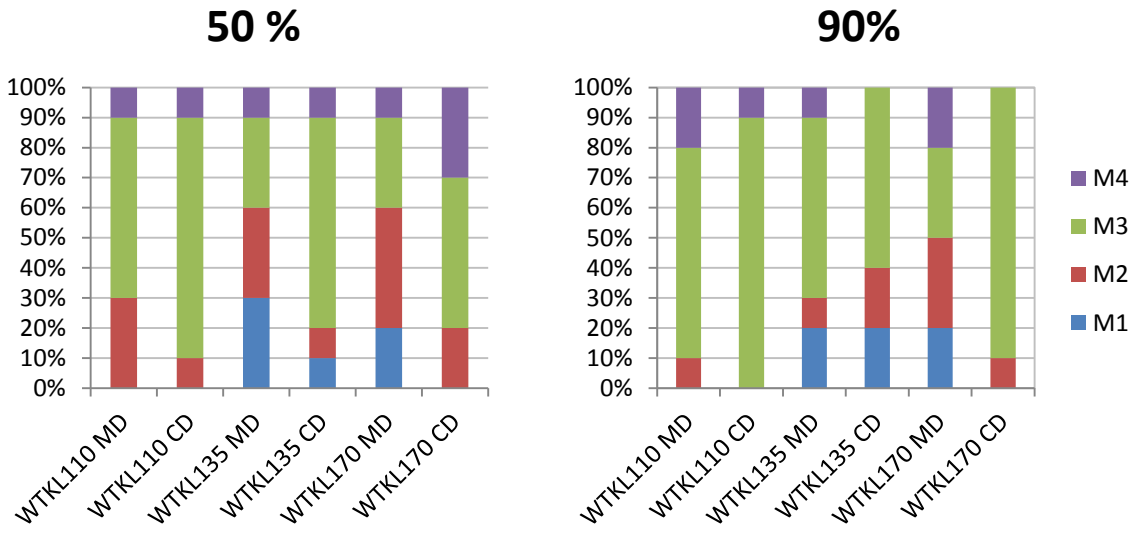

Figure 4.12. Distribution of the failure modes in WTKL for both 50% and 90%RH.

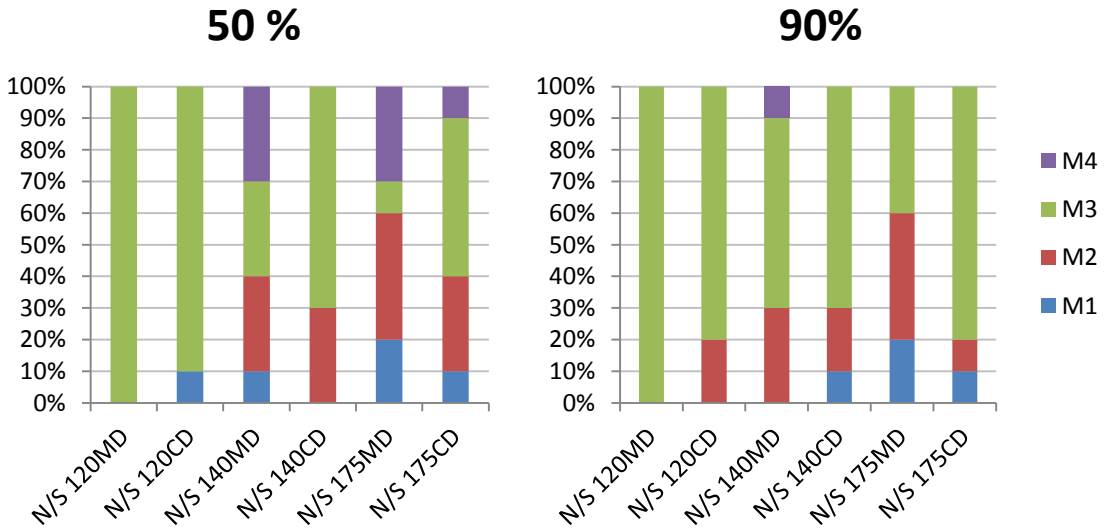

Figure 4.13. Distribution of the failure modes for the N/S medium 50% and 90% RH.

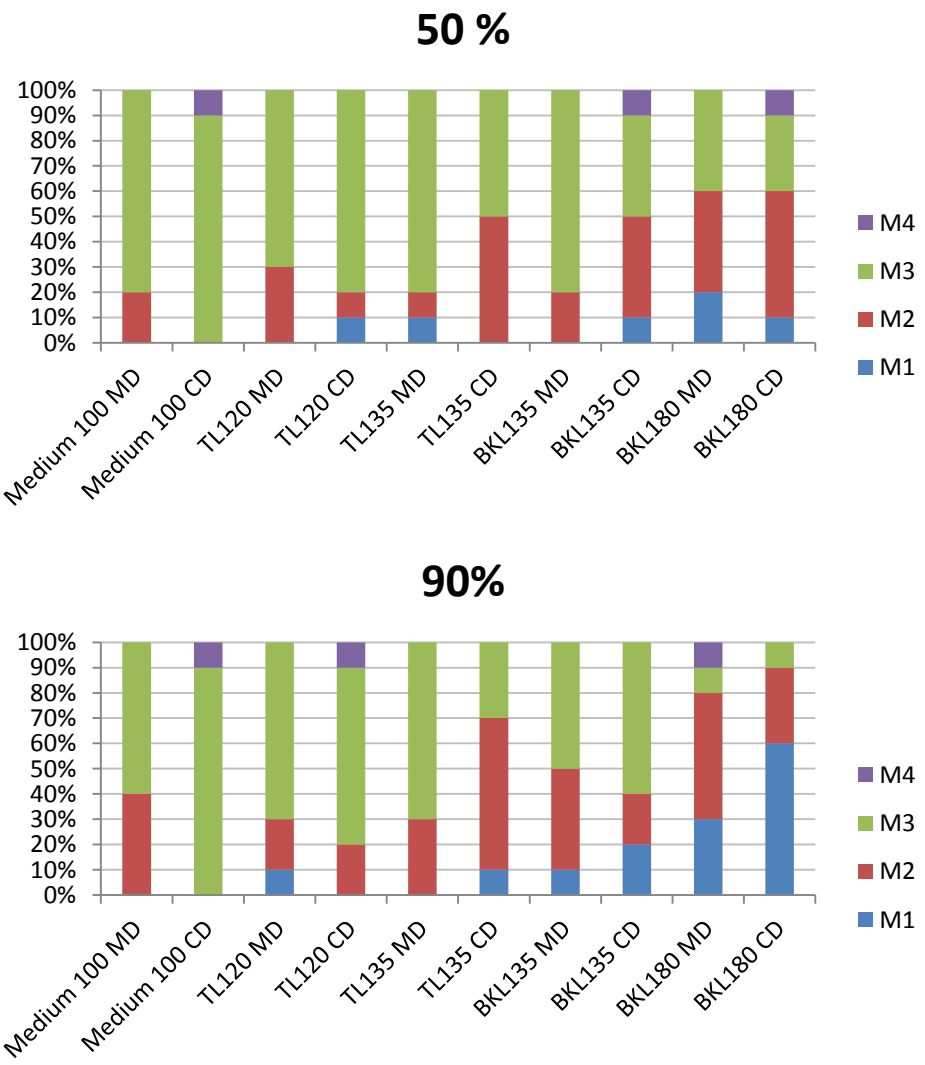

Figure 4.14. Distribution of the failure modes for the recycled materials at both 50% and 90% RH.

When studying the distribution of the different types of failure modes for the different qualities no trend can be seen between papers conditioned at 50% RH and 90% RH, which was unexpected. As discussed in section 2.4, humidity reduces the tensile stiffness of the fibres, which is an important parameter in the Euler's model for buckling. A shift towards M3 failure modes was therefore expected and some materials (WTKL170CD, N/S 175 MD and CD) showed that trend. But when comparing with the other qualities and grammages, no general trend can be seen and the different failure modes could be due to the random behaviour of the fibre network. As stated earlier, a plausible explanation is that the swelling of the fibres counteracts the change in the stiffness due to the increase of the samples thickness. For the lower grammages, M3 was the dominant type of failure for all types of paper material, and especially for the low weight qualities.

Hansson's study (2013) covered materials in the range of 170 g/m^2 up to 400 g/m^2 of different types of paperboard. When comparing the results from this study with Hansson's, the results for low grammage solid boards showed similar results.

The virgin based materials experienced more M4 failures than the recycled based materials. The M4 failures can be due to the fibre network being too stiff and strong for the clamps to be able to cause a complete failure in the paper. Observation of the failure area of samples that were registered as a M4

mode showed signs of failure that had not travelled throughout the entire width of the sample, but had a normal force-displacement curve which implies a complete failure in the paper. This implies that the failure mode has not propagated throughout the entire width of the sample and the measured strength is due to a different failure mode. This implies that the failure could be one of the other three failure modes. The M4 failures could also be due to differences in the friction between the clamps and the sample, depending on the quality studied. Observations of the recordings showed less sliding between the clamps for recycled based materials. To investigate if the friction coefficient of the paper could be linked to the sliding between the clamps, the friction angle was measured on all paper qualities. The results can be seen in *Table 4.5*.

Table 4.5. friction angle for the different materials.

WTKL	N/S	BKL	RBF	TL
29.0°±3.8°	20.0°±2.5°	24,8°±4.4°	20.2°±3.0°	22.0°±1.5°

Sliding was observed for all samples and qualities, some qualities to a greater extent than other. As *table 4.5* shows there is small differences between the different materials. When studying the distribution of the different failure modes in *Fig. 4.13-4.15*, no direct correlation can be seen between the friction angle and the number of M4 failures, implying that the failures mostly occur due to the random behaviour of the fibre network. However, for future studies the friction against a metallic surface could result in different friction constants and give a better explanation on how the sliding affects the SCT measurements as well as what exactly the SCT machine measure and if a M3 failure mode should be considered as a compression failure.

4.2.3. SCT Correlation between failure modes and the strength/stiffness of the material

Fig. 4.15 and *4.16* shows the distribution of the failure modes plotted against corresponding compression stiffness- and strength index. Because no correlation was found for neither the strength nor the stiffness for any of the covered materials only two are reported in the discussion. Remaining graphs are found in appendix III.

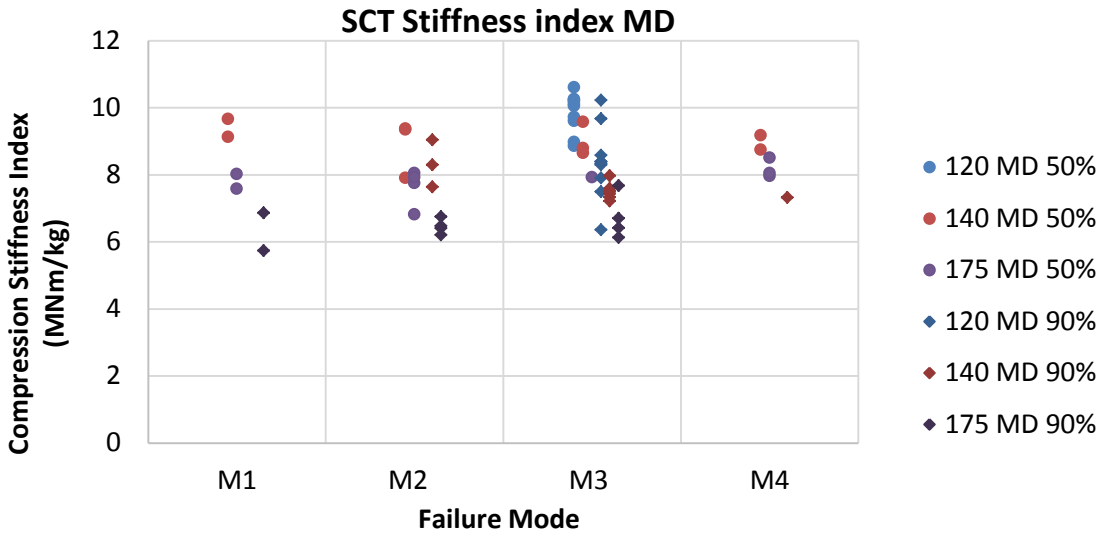

Figure 4.15. Failure modes for N/S fluting plotted against the corresponding stiffness for the samples. The different series contain ten samples each.

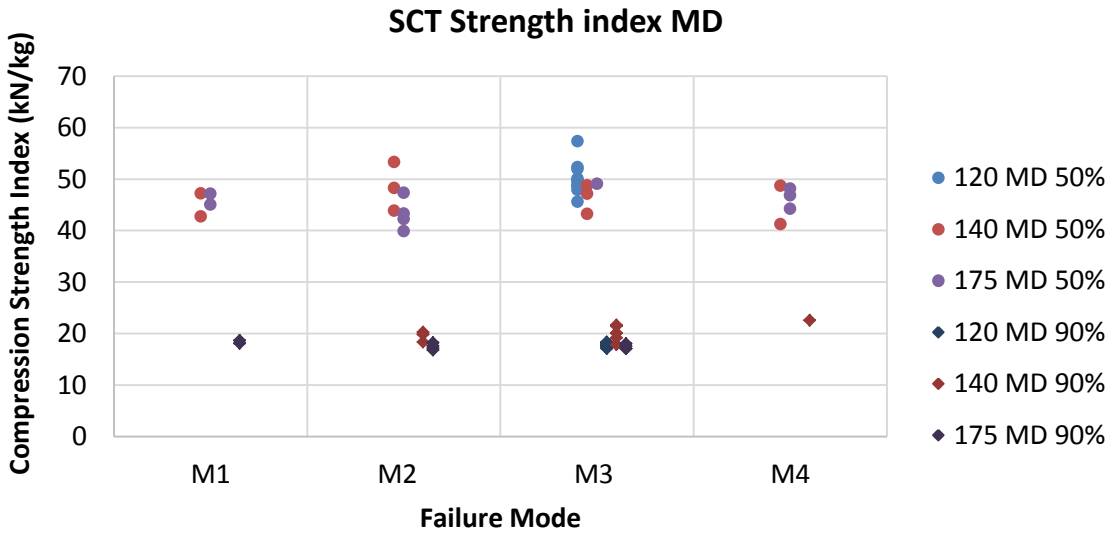

Figure 4.16. Failure modes for N/S fluting plotted against the corresponding strength for the samples. The different series contain ten samples each.

As *Fig. 4.15* and *4.16* show that no correlation can be found for the type of failure mode and the corresponding strength or stiffness of the sample. In *Fig. 4.16*, paper conditioned at 50% holds a higher stiffness than paper conditioned at 90% RH. For the compression strength the difference between the two RH conditions were more pronounced with a clear difference between 50% and 90% and are in line with earlier studies by Chalmers (1998), Page (1969) and Back et al. (1983).

The lack of correlation between the strength/stiffness and the type of failure mode is good when considering the everyday testing of paper. If there had been a difference between the types of modes each sample would have to be studied, which would make the method more time consuming. For this study, these results further prove that there is an uncertainty in how the compression is evaluated as there is no clear connection between a pure compression failure and a bending failure, expected for thin papers.

4.3. Influence of humidity

4.3.1. Grammage, thickness and density

Fig 4.17-4.19 show how the paper parameters change when the material is conditioned at 50% and 90% RH.

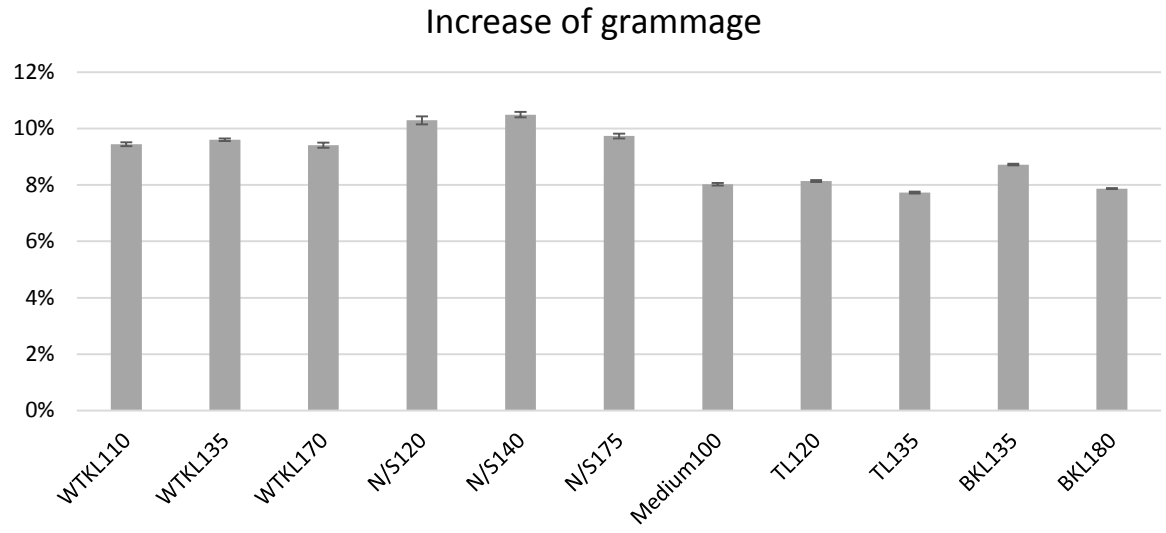

Figure 4.17 . Increase in the grammage for the materials when conditioned at 90% compared to 50%.

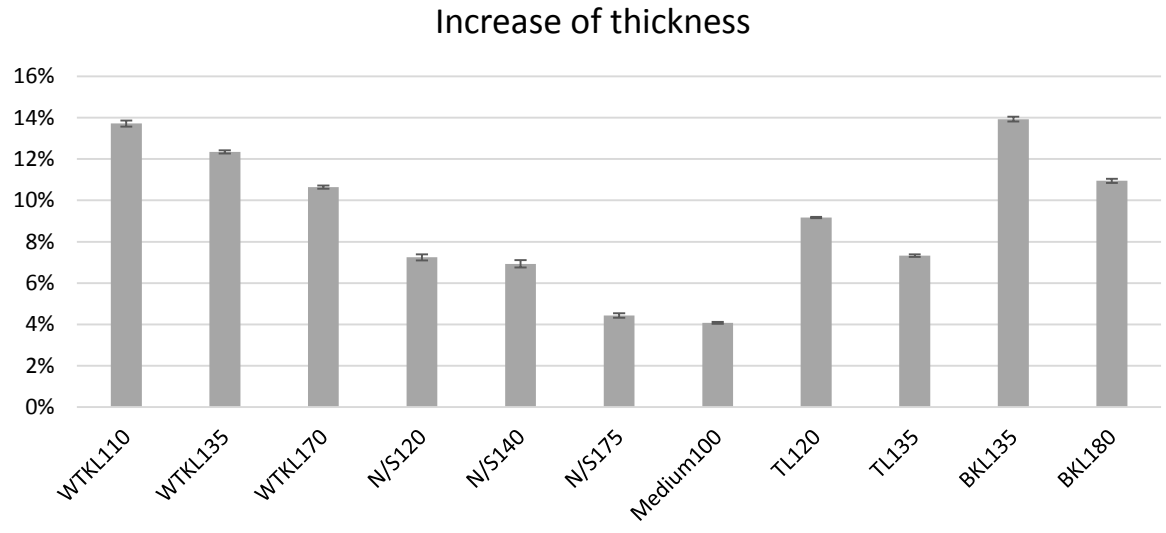

Figure 4.18. Change of the thickness in the materials when conditioned at 90% compared to 50%.

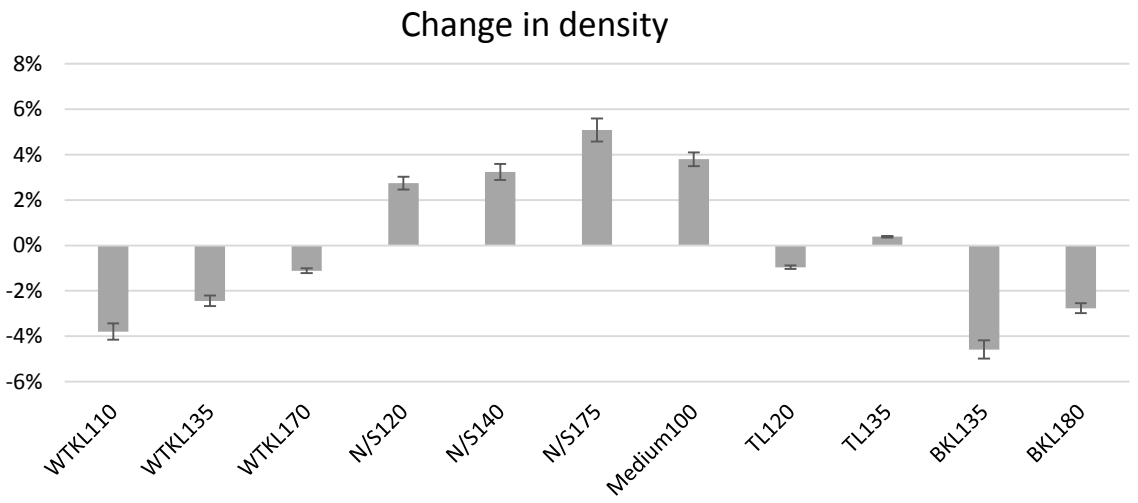

Figure 4. 19. Change in density for the materials when conditioned at 90% and 50%.

As Back et al. (1983), Chalmers (1999) and Navaranjan et al. (2012) discussed in the literature, the increased presence of water vapour in the air will result in dimensional changes of the fibre network. In *Fig.4.19* it is clear that the virgin based material adsorbs more moisture then the recycled materials, which supports the findings of Zhang et al. (2001). When considering the change in the thickness the linerboard materials showed a greater increase than the medium materials. For the N/S fluting, it is possible that the hydrophobic lignin in the fibres protect the hemicellulose and cellulose chains from the water molecules, with the water molecules being attached only to the surfaces of the fibres. For the recycled medium the small change is related to how many times the fibres have been recycled as the recycling process and drying process affect the fibres ability to swell and that the swelling that occurs is due to the starch. *(Navaranjan et al. 2012)*

When considering the density changes, the fluting mediums express a higher density at 90% RH than at 50%. The linerboards showed the opposite trend and experienced a decrease in density. When related to the change in the thickness and grammage the decrease of the density was expected. Why the increase in the grammage does not reflect on the change in thickness in the fluting materials, suggests that not all water present in the fibre network causes swelling of the fibres, thus resulting in an increase in density.

4.4. Determination of the moisture content in paper and the effects on SCT performance

Table 4.5 show the results from the RH study with both the RH according to literature and the RH acquired in the sealed jar.

Table 4.5. The achieved RH from the salt solutions.

Salt	Desired RH	Measured RH
Dry	0%	0%
Magnesium Chloride ($MgCl_2$)	33%	46.8%
*Reference	50%	50.1%
Sodium chloride (NaCl)	75%	77.4%
Ammonium chloride ($(NH_3)_2SO_4$)	80%	82.9%
Potassium chloride (KCl)	85%	85.2%
Barium dichloride ($BaCl_2$)	90%	95.5%
Potassium Nitrate (KNO_3)	95%	86.9%

Magnesium chloride and KNO_3 did not give of the desired RH. For the $MgCl_2$ solution this is most likely due to the solution being unsaturated. The values of KNO_3 stands out as the desired RH is significantly higher than the achieved RH, but the moisture content in the sample and the measured SCT value, appears to follow the adsorption curve and performance curve reported by Fellers and Bränge (1985). $BaCl_2$ gives of a high value in the RH compared to the desired RH, but it can be due to the uncertainty in the instrument (±3%). As the instrument was not suitable for measurements over 95% RH it can explain the odd result for the KNO_3. The high value of water can be due to condensation on the sensor, resulting in the surface being saturated with water molecules.

Due to the uncertainty in the measurements of the high level RH salts the results are plotted against the desired values of the RH. For the measured RH against SCT see *Fig. A-I.1* in appendix I.

Fig. 4.20 shows the SCT performance against the desired relative humidity. $MgCl_2$ was excluded from the graph due to being unsaturated and thus not correlating to the desired value of the RH. All values where normalised against the SCT value at 50% RH to illustrate the differences between the materials

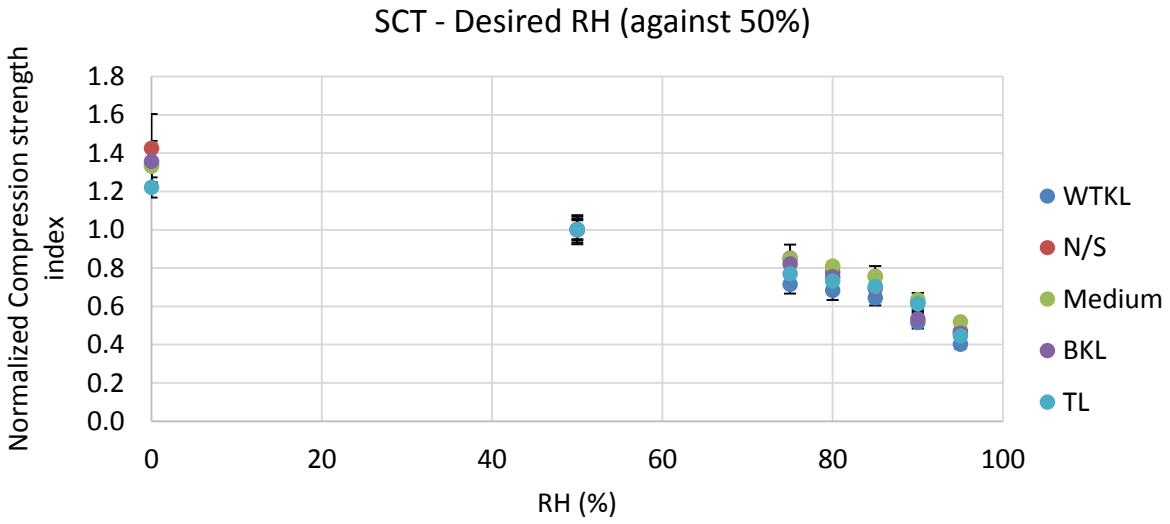

Figure 4.20. Shows how the SCT value depends on the desired relative humidity.

As *Fig 4.21* show the SCT value decreases with increased RH. There is no significant difference between the samples conditioned in the "dryer" climate with $MgCl_2$ due to the small difference in the archived RH of 46.7% and the samples conditioned at 50% RH. For the samples conditioned for the salts at higher levels of RH they trend to decrease. There is however hard to tell if there is a significant difference between the SCT values at 95% and 98% RH. The results are consistent with results reported by Fellers and Bränge (1985). *Fig 4.24* shows the moisture content in the paper as a function of the relative humidity. As the RH increases, so will the moisture content in the fibre network. WTKL was observed to adsorb significantly less moisture than the other materials. The increased amount of moisture correlates to the decrease of the SCT value seen in *Fig.4.20* and the results is consistent with reported literature *(Benson 1971).*

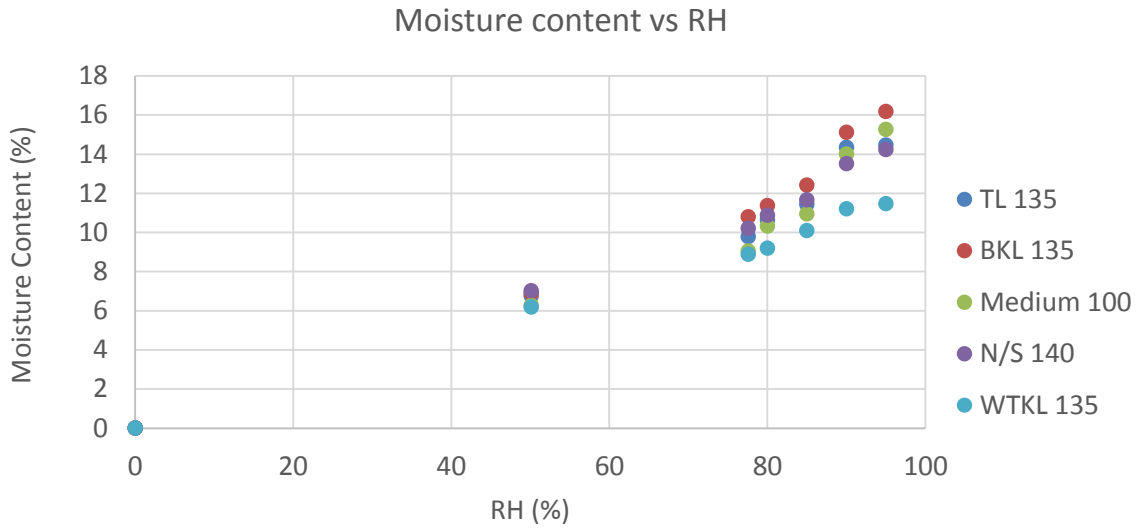

Figure 4. 21 Moisture content in the paper plotted against RH

Why the WTKL appears to adsorb the least moisture, when the literature state that virgin materials adsorb more moisture, could be because it holds low levels of fines and other small particles. As discussed earlier recycled fibres contain starch, but does also contain higher levels of fines and other particles. Together with the hydrophilic starch, these small particles increase the total area of where moisture can be adsorbed to causing an increase of the moisture content in the paper. It would therefore be interesting to investigate how the relative humidity affect paper containing different amount of starch to see if the moisture content increase with an increased amount of starch, in addition to how the strength and stiffness is affected.

5. Conclusion

5.1. Principal findings

The findings in this study can be summarised in a couple of points which track back to one of the three main objectives.

For the first objective consisting of the investigation of how the failure mechanisms in compression and tensile proceeds, the results show that there is a difference between the two methods. While the compression stiffness and tensile stiffness is considered to be the same at 50% RH there was in most cases a difference between the stiffnesses at 90% RH. It is generally known that the strength is lower in compression than in tension at 50% RH and there is a difference at 90% as well. This is also caused by the different methods used for evaluating the strength and stiffness properties of the paper.

- The mechanism that governs the tensile failure can be related to the fibre networks properties while the mechanism related to compression is governed by the properties of the individual fibres.
- Due to the uncertainty in the testing method, it still remains unclear of what exactly causes the fibre network to fail in true compression failure rather than in a buckling failure.
- The SCT method for evaluating the compression of the paper network does not give a true value of the compression strength and stiffness in the paper.

The SCT machine used for evaluating the compression properties for the materials does not differentiate between the different types failure modes identified by Hansson (2013), i.e. the machine does not detect if there is a buckling or shearing failure in the paper. Recordings of the failures do however show that no correlation can be seen between the type of failure and the corresponding stiffness or strength value. These results are promising for continued usage of the SCT method for every day product control but do not contribute to the development of a better understanding of the true compressive response in the paper.

Considering the humidity's influence on the strength and stiffness properties of the paper, following conclusion have been made.

- The strength and stiffness values for virgin based materials are superior to that of recycled materials at both 50% RH and 90% RH.
- In this study the compression stiffness was higher than the tensile stiffness at 90% RH.
- No change in the distribution of different failure modes were observed in SCT when samples were conditioned at 90% RH rather than 50% RH.

5.2. Future work

A topic for future studies is the relation between the papers anisotropy and the retention of the strength and stiffness properties in the paper by using the same method presented in this study on handmade lab sheets with different anisotropy.

Another suggestion for future work is to study the influence of humidity on starch present in paper materials, discussed in paragraph 4.1.3. A possible example is how different volumes of starch added to pulp will influence the papers performance at 50% compared to 90% RH. A study could also

include how much the moisture content in the paper increases with varying volumes of starch in the paper.

Further evaluation of the actual compression of the paper would give a better understanding of the failure mechanisms that affect in compression test. Maybe it would be possible to develop a compression testing method that can be used in combination with the Zwick/Roell equipment. In addition, it would be necessary to investigate if a certain type of failure mode in SCT can be correlated to the friction or surface topography of the paper sheet.

Lastly this study could be extended to include the correlation between the humidity and the creep behaviour in the paper.

6. References

Back E.L., Salmén L. and Richardson G., (1983), Transient effects of moisture sorption on the strength properties of paper and wood-based materials, Svensk Papperstidning, 86(6) 61-71.

Benson R.E. (1971) Effects of relative humidity and temperature on tensile stress-strain properties of Kraft linerboard, Tappi, 54(5) 699-703.

BillerudKorsnäs – Homepage, (2016-05-23) http://www.billerudkorsnas.com/en/About-Us/

Borgqvist E, Wallin M, Ristinmaa M, Tryding J and Tudisco E, (2016) Localized deformation in compression and folding of paperboard, Packaging technology and science, Under review.

Brännvall E. (2009), The Ljungberg textbook, Volume 2, Pulping chemistry and technology, Chapter 1 Overview of pulping and paper processes. Berlin: Walter de Gruyter Gmbh & Co.

Brännvall E. (2009b), The Ljungberg textbook, Volume 2, Pulping chemistry and technology, Chapter 6 Chemical pulping. Berlin: Walter de Gruyter Gmbh & Co.

Chalmers I.R. (1998), The effect of humidity on packaging grade paper elastic modulus, Appita Journal, 51(1) 25-28.

Dahlgren, L., Olsson, L. and Danielsson, O. (1980): Halvkemiskt massa, neutralsulfit-tillverkning, 2nd edition, Markaryd: Sveriges skogsindustriförbund, in Swedish.

Daniel, G. (2009), The Ljungberg textbook, Volume 1 Wood Chemistry and Wood Technology, Chapter 3 Wood and Fibre Morphology, Berlin: Walter de Gruyter GmbH & Co.

Demitrov K. and Heydenrych M., (2009), Relationship between the Edgewise compression strength of corrugated board and the compression strength of liner and fluting medium papers, Southern Forests: a Journal of Forest Science, 71(3) 227-233.

Eklund D. and Lindström T., (1991), Paper Chemistry: an introduction, Chapter 2, Grankulla: DT PAPER SCIENCE, Finland.

Engstrand P and Johansson B. (2009), The Ljungberg textbook, Volume 2, Pulping chemistry and technology, Chapter 15 Paper Recycling. Berlin: Walter de Gruyter Gmbh & Co.

ERPC – European Recovered Paper Council (2016-05-06), http://www.paperrecovery.org/paper-recycling.

Fellers C., (1986) Paper Structure and Properties, Chapter 14 the significance of structure for the compression behaviour of paperboard. New York: Marcel Dekker, inc.

Fellers C., (2010), The Ljungberg textbook, Volume 4, Paper Products Physics and Technology, chapter 2 Paper Physics, Berlin: Walter de Gruyter Gmbh & Co.

Fellers C. and Gimåker M., (2011) Literature review on in-plane compressive properties of paper. Innventia Report.: 154

Fellers C. and Bränge Å., (1985) The impact of water sorption on the compression strength of paper, London: Mechanical Engineering publications. 1985 (2) 529-539.

Frank B., (2014), Corrugated box compression – a literature survey, Packaging technology and science, 2014(27) 105-128.

Gullerstedt G. (2009), The Ljungberg textbook, Volume 2, Pulping chemistry and technology, chapter 5, Chemistry of chemical pulping. Berlin: Walter de Gruyter Gmbh & Co.

Gullichbsen, J. and Fogelholm C.J. (2000), Chemical Pulping 6A, Chapter 2, fibre line operations, Jyväskylä: Fapet Oy.

Grafiska Yrkesnämden (1983), compendium: Wellpapp – Tillverkning, first edition, Näringslivets förlagsdistrution, Stockholm. In Swedish.

Greenspan L., (1976) Humidity fixed points of binary saturated aqueous solutions, Journal of Research, 81(1) 89-96.

Gunderson D.E., Considine J.M. and Scott C.T. (1988), Journal of pulp and paper science, 14(2) 37-41.

Hagman A., Huang H. and Nygårds M. (2013) Investigation of shear induced failure during SCT loading of paperboards, Nordic Pulp and Paper Research Journal, 28(3) 415-429

Hansson B., (2013), Evaluation of compression testing and compression failure modes of paperboard. Master thesis, department of engineering and chemical sciences, chemical engineering, Karlstad University.

Henriksson G., (2009) The Ljungberg textbook, Volume 1 Wood Chemistry and Wood Technology, Chapter 6 Lignin, Berlin: Walter de Gruyter Gmbh & Co.

Höglund H., (2009), The Ljungberg textbook, Volume 2, Pulping chemistry and technology, chapter 4 Mechanical pulping. Berlin: Walter de Gruyter Gmbh & Co.

ISO 534:2011 Paper and board -- Determination of thickness, density and specific volume

ISO 536: 2012 Paper and board -- Determination of grammage

ISO 1924-3:2011, Paper and board - Determination of tensile properties - Part 3: Constant rate of elongation method (100 mm/min).

ISO 9895:2009, Paper and board – Compressive strength – short span test.

Kajanto I. (1998), Papermaking Science and Technology, Book 16 Paper Physics, Chapter 6 Structural mechanics of paper and board, Jyväskylä: Fapet Oy Finland.

Kajanto I and Niskanen K (1998) Papermaking Science and Technology, Book 16 Paper Physics, Chapter 7 Dimensional stability, Jyväskylä: Fapet Oy Finland.

Kolseth P. and de Ruvo A. (1986) Paper Structure and Properties, Chapter 1 The cell wall components of wood pulp fibers. New York: Marcel Dekker, inc.

Lennholm L. and Henriksson G. (2009) The Ljungberg textbook, Volume 1 Wood Chemistry and Wood Technology,, Chapter 4 Cellulose and Carbonhydrate Chemistry, Berlin: Walter de Gruyter Gmbh & Co.

Lindström T. (1986) Paper Structure and Properties, Chapter 4. The concept and measurement of fibre swelling, New York: Marcel Dekker, inc.

Levlin J. (1999), Papermaking Science and Technology, Book 17 pulp and paper testing, Chapter 7 General physical properties of paper and board, Jyväskylä: Fapet Oy Finland

Markström H. (1999), Testing methods and instruments for corrugated board, Stockholm: Lorentzen & Wettre. p. 75-77.

Mäkelä P. (2010), In-plane compression properties for selected commercial papers. Innventia Report no; 76.

Navaranjan N., Dickson A., Paltakari J. and Ilmonen K. (2012) Humidity effect on compressive deformations and failure of recycled and virgin layered corrugated paperboard structure, Composites: part B, 45(2013) 965-971.

Norman B. (2009). The Ljungberg textbook, Volume 2, Pulping chemistry and technology, Chapter 10-11 Web forming and Wet pressing. Berlin: Walter de Gruyter Gmbh & Co.

Page D. H. (1969), A theory of the tensile strength of paper, TAPPI Journal 52(4) 674-681.

Richardson S. and Gorton L., (2003), Characterisation of the substituent distrubution in starch ans cellulose derivatives. Analytica Chimica Acta, 497(1-2) 27-65.

Rigdahl M. and Hollmark H., (1986), Paper structure and properties, chapter 12 Network Mechanics. New York: Marcel Dekker, inc.

Retulainen E., Niskanen K. and Nilsen N. (1998), Papermaking Science and Technology, Book 16 Paper Physics, Chapter 2 Fibres and bonds, Jyväskylä: Fapet Oy Finland.

Niskanen K and Kärenöampi P, (1998), Papermaking Science and Technology, Book 16 Paper Physics, Chapter 5, In-plane tensile properties, Jyväskylä: Fapet Oy Finland.

Rhim J-W, (2010), Effects of moisture content on tensile properties of paper-based food packaging materials, Food Science Biotechnologies, 19(1), 243-247.

Rockland L.B., (1960) Saturated salt solutions for static control of relative humidity between 5° and 40°C. Analytical Chemistry, 32(10) 1375-1376.

Räisänen V. I., Alava M. J., Nieminen R. M. and Niskanen K. J., (1996), Elastic-plastic Behaviour in fibre networks, Nordic Pulp and Paper Research Journal, 11(4) 243-248

Shallhorn P., Ju S. and Gurnagul N., (2004), A model for short-span compressive strength of paperboard, Nordic Pulp and Paper Research Journal, 19(2) 130-134.

Sjöström E. (1981), Wood Chemistry: fundamentals and applications. Chapters 1, 3, 4, 5 and 7. London: Academic Press inc.

Söremark C. and Tryding J. (2009), The Ljungberg textbook, Volume 4, Paper Products physics and technology, Chapter 10 Packaging. Berlin: Walter de Gruyter Gmbh & Co.

Teleman A. (2009),The Ljungberg textbook, Volume 1 Wood Chemistry and Wood Technology, Chapter 5 Hemicellulose and Pectins, Berlin: Walter de Gruyter Gmbh & Co.

Wahlström T., (2010) The Ljungberg textbook, Volume 4, Paper Products physics and technology, Chapter 46 Development of paper properties during drying. Berlin: Walter de Gruyter Gmbh & Co.

Wink W.A. Watt J.A. Whitsitt W.J. and Baum G.A. (1984), Role of fibre axial modulus on compressive strength, Fibre Science and Technology 20(4) 245-253.

Zhang M., Hubbe H. A., Venditti R. A. and Heitmann J. A. (2001) Effect of chemical pretreatments of never- dried pulp on the strength of recycled linerboard. Proc. Tappi 2001 Papermakers conf. digital doc.

Appendix I

Table A. 1 Lists all calculated α_{SCT} quotes used for rescaling the SCT curves.

	MD	CD
WTKL		
110 g/m²	0.049	0.109
135 g/m²	0.064	0.104
170 g/m²	0.060	0.085
TL		
120 g/m²	0.083	0.117
135 g/m²	0.077	0.128
BKL		
135 g/m²	0.061	0.119
180 g/m²	0.051	0.096
N/S		
120 g/m²	0.055	0.104
140 g/m²	0.053	0.100
170 g/m²	0.051	0.092
Medium		
100 g/m²	0.083	0.145

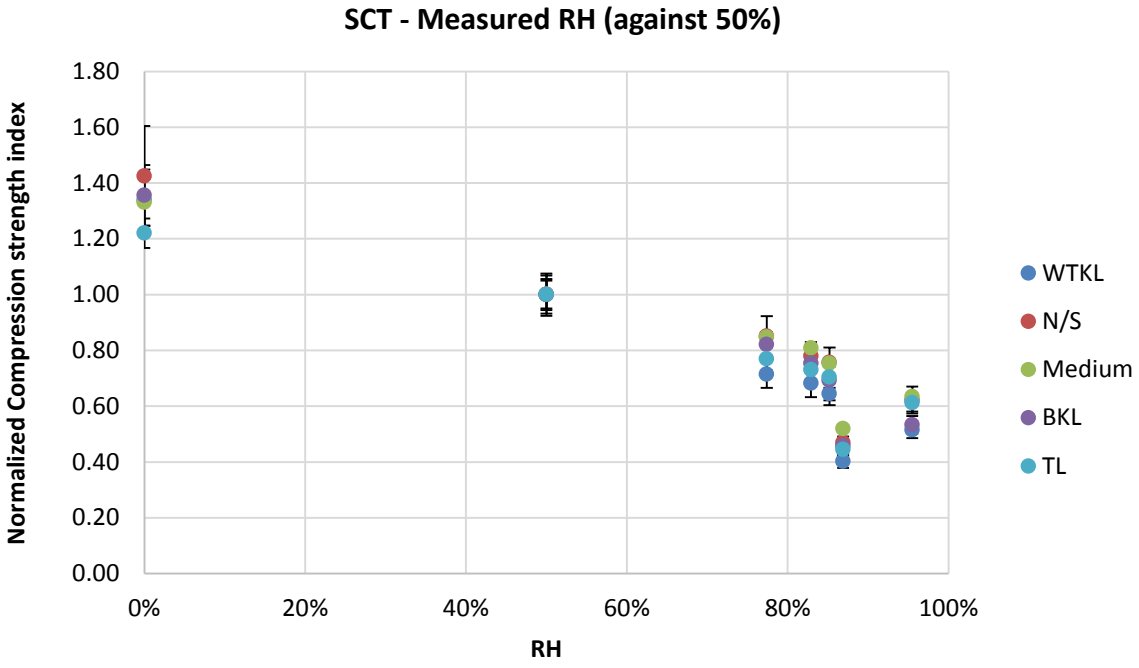

Figure A-I.1 desired RH against SCT.

Appendix II

Fig. A-II.1 to A-II.6 show the absolute stiffness and strength values in both tensile and compression for all linerboard materials.

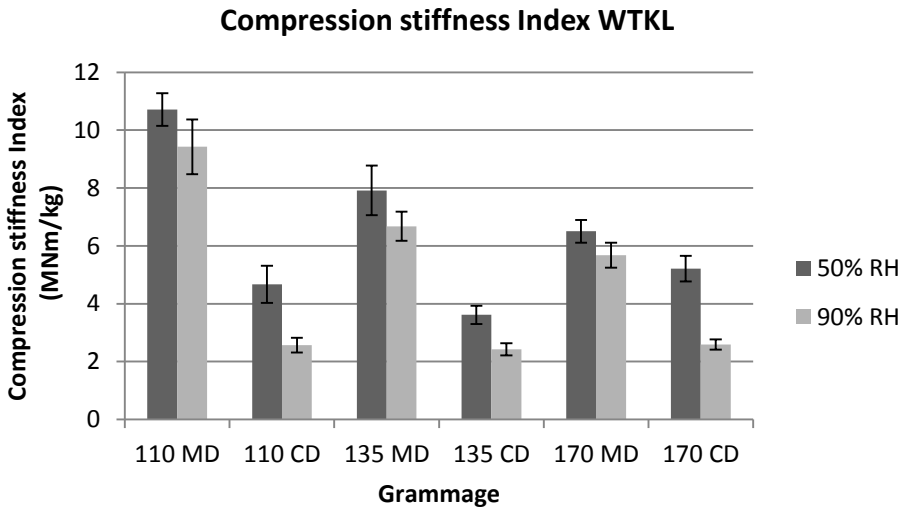

Figure A-II.1 Absolute values of the compression stiffness index for WTKL.

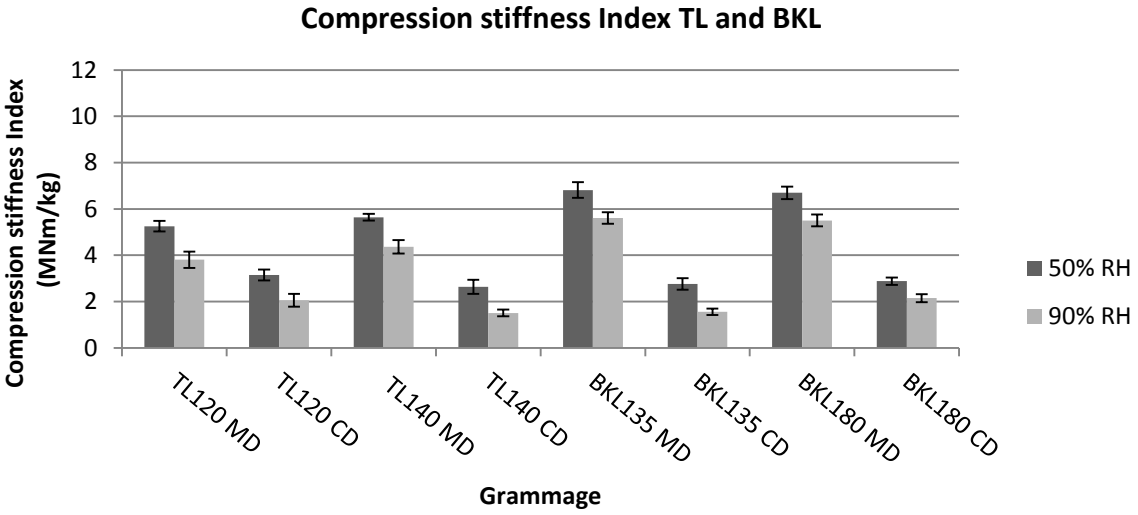

Figure A-II. 2. Absolute values of the compression stiffness index for TL and BKL.

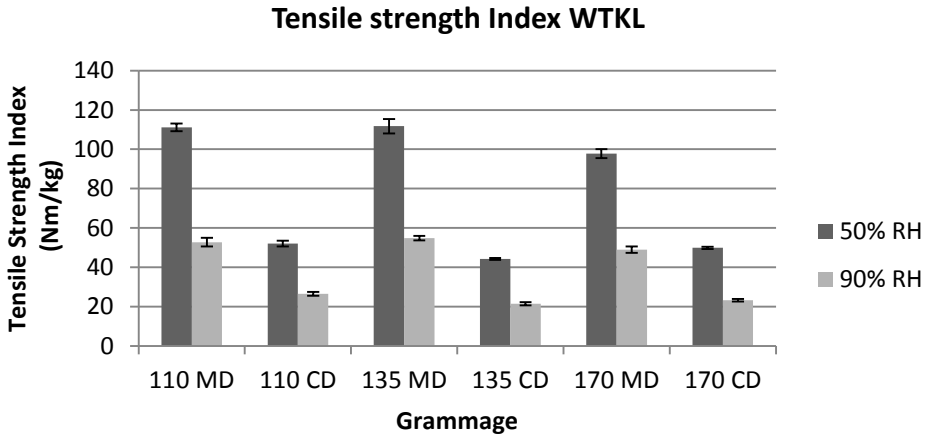

Figure A-II. 3 Absolute values of the tensile strength index for WTKL

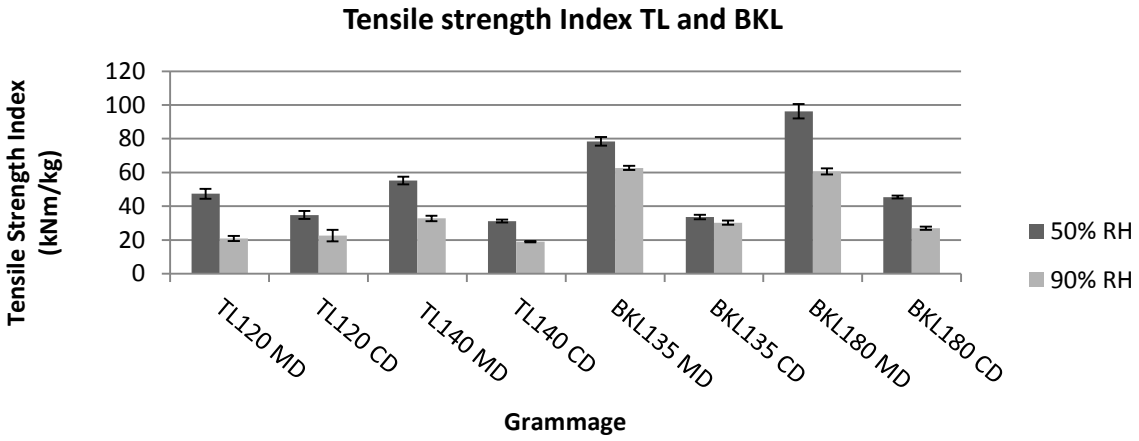

Figure A-II. 4. Absolute values of the tensile strength index for TL and BKL

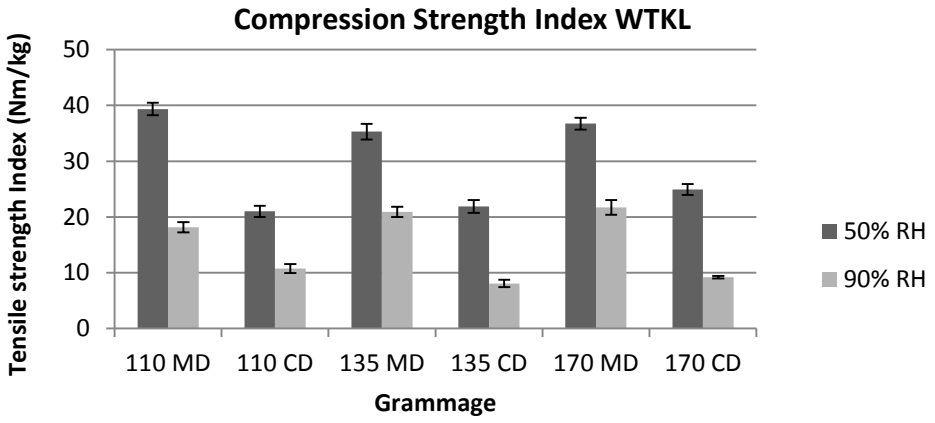

Figure A-II. 5. Absolute values of the compression strength index for WTKL

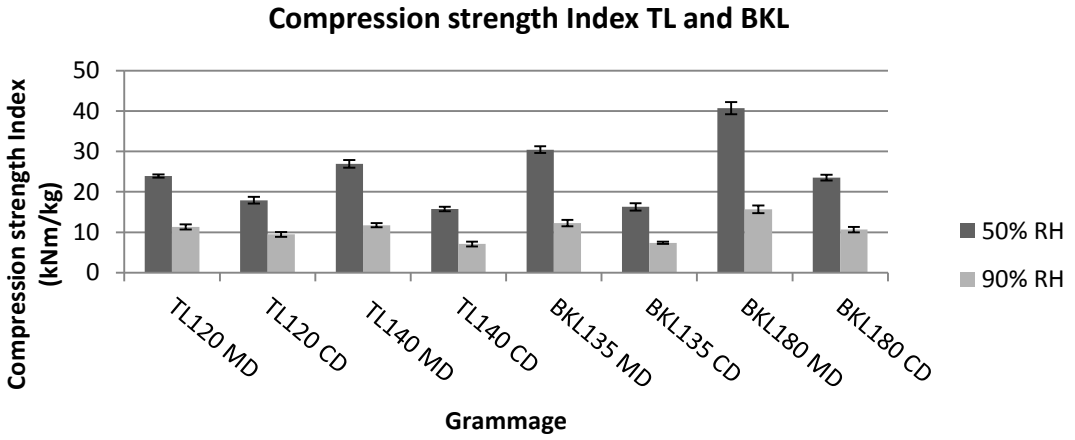

Figure A-II. 6. Absolute values of the compression strength index for recycled linerboards

Fig. A-II.7–A-II.14 Show the Absolute tensile and stiffness values for N/S fluting and recycled medium in both compression and tensile.

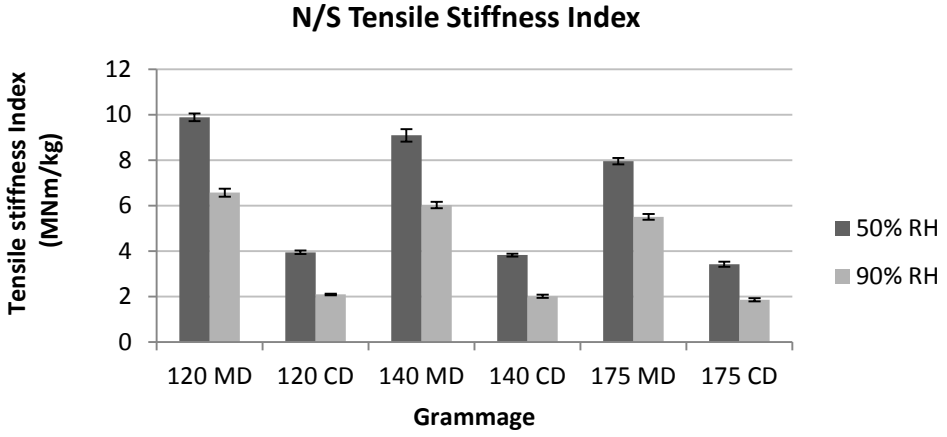

Figure A-II.7. Absolute values of the compression stiffness index for N/S.

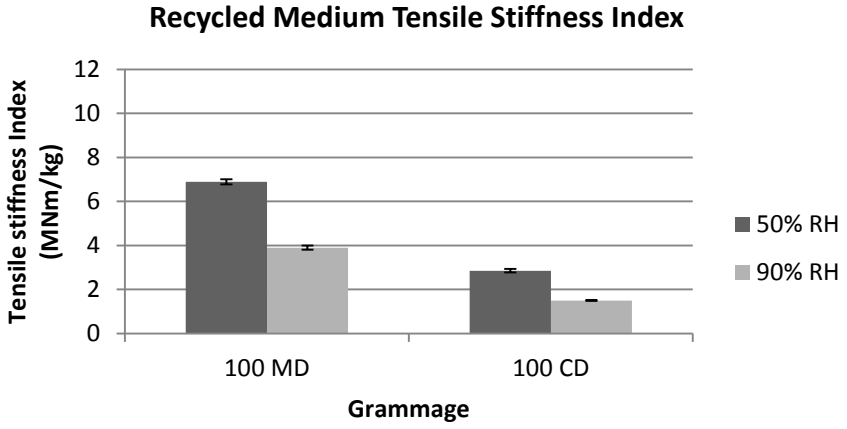

Figure A-II. 8. Absolute values of the tensile stiffness index for recycled Medium.

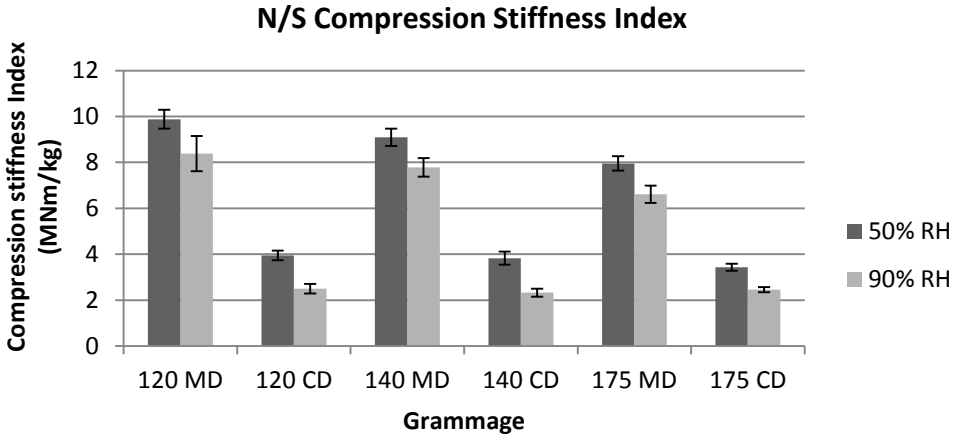

Figure A-II. 9. Absolute values of the compression stiffness index for N/S

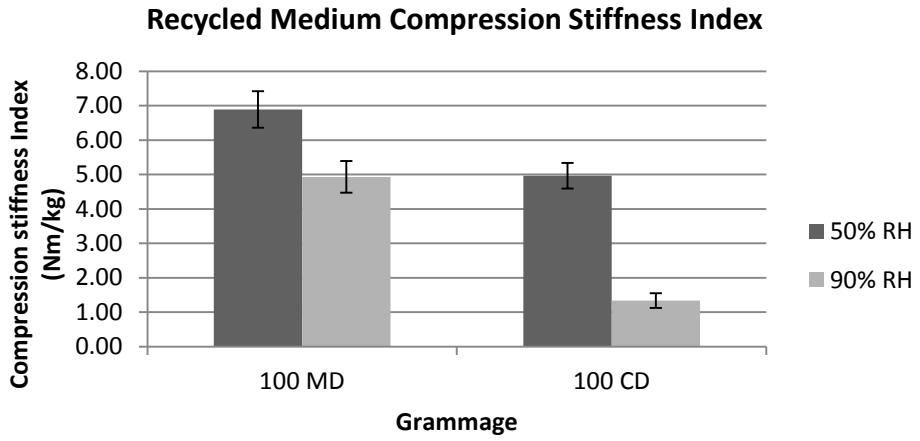

Figure A-II. 10. Absolute values of the compression stiffness index for recycled Medium.

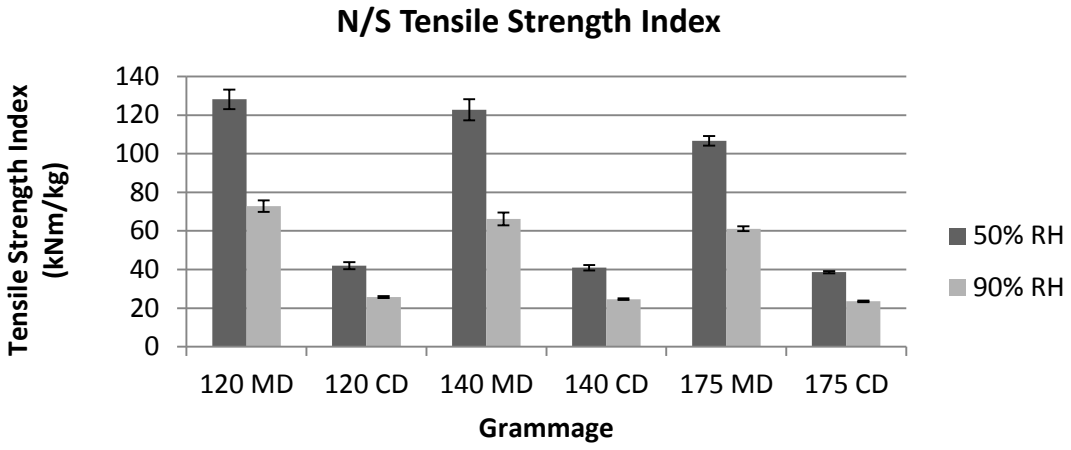

Figure A-II. 11. Absolute values of the tensile strength index for N/S.

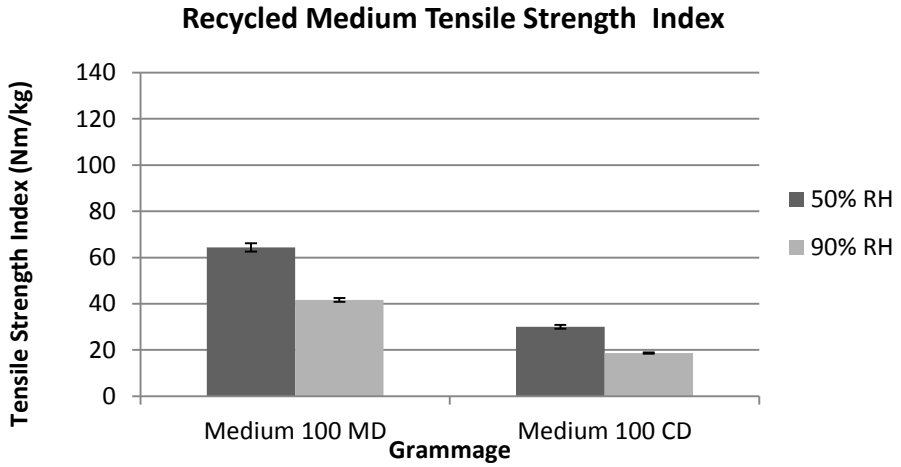

Figure A-II. 12. Absolute values of the tensile strength index for recycled Medium.

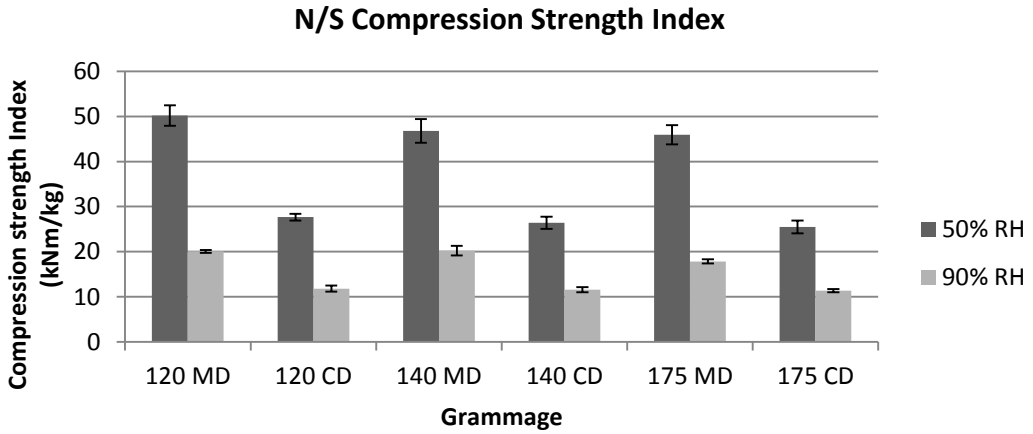

Figure A-II. 13. Absolute values of the compression strength index for N/S.

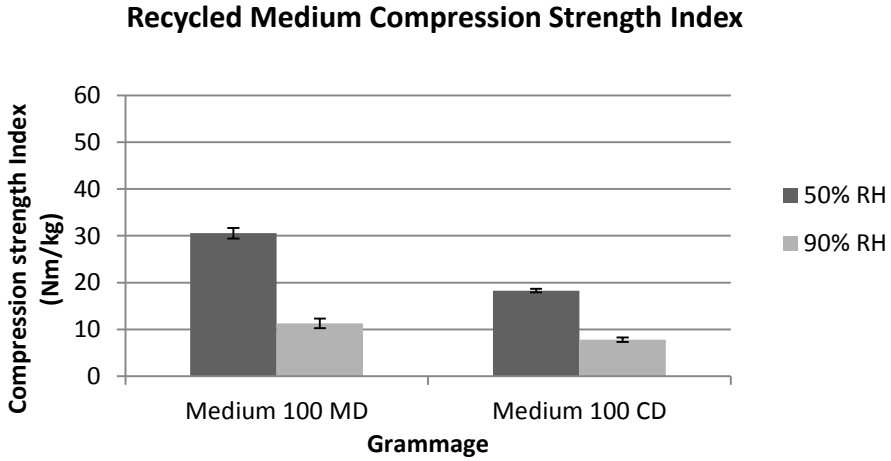

Figure A-II.14. Absolute values of the compression strength index for recycled Medium.

Appendix III

Fig. A-III.15-A-III.28 Represent the distribution of failure modes plotted against their corresponding stiffness and strength values.

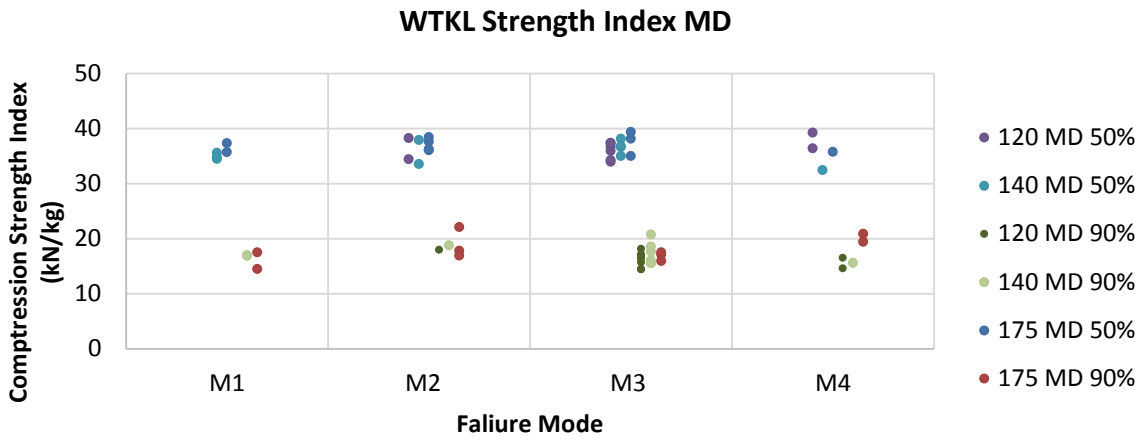

Figure A-III. 15

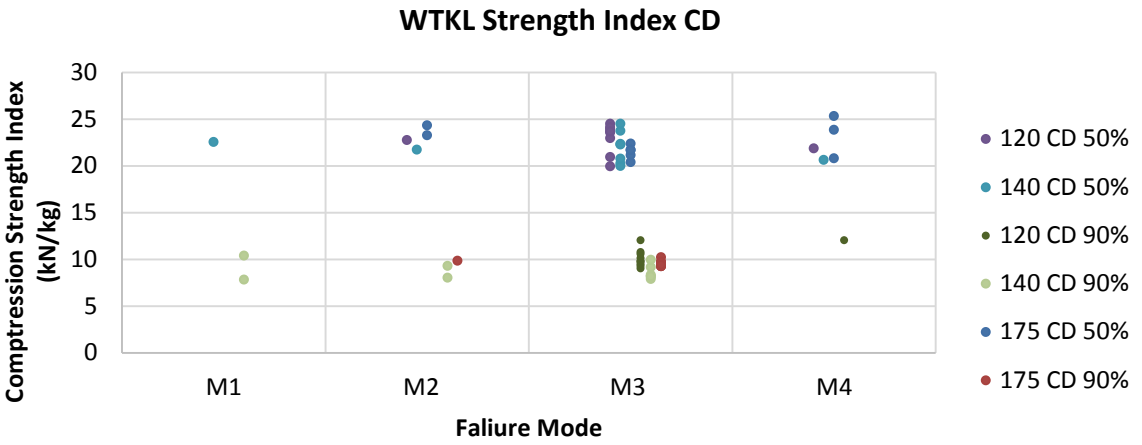

Figure A-III. 16

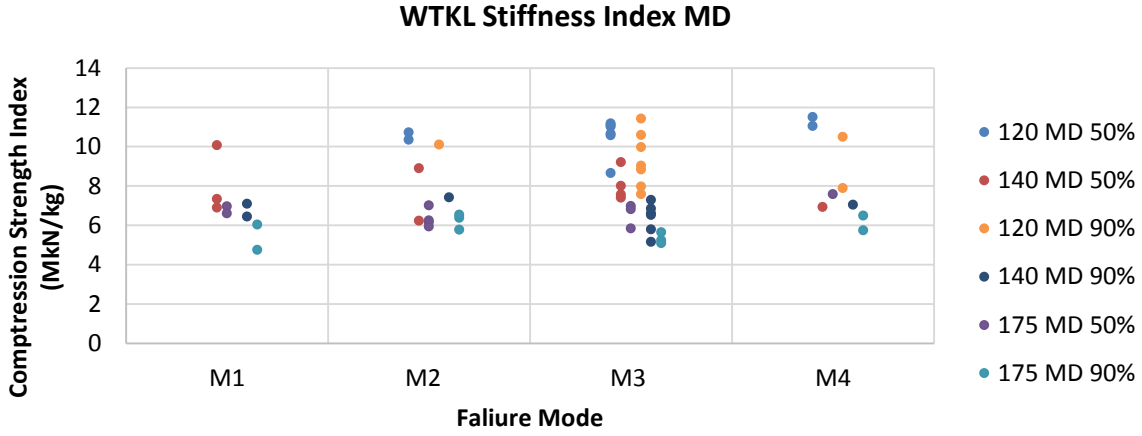

Figure A-III. 17

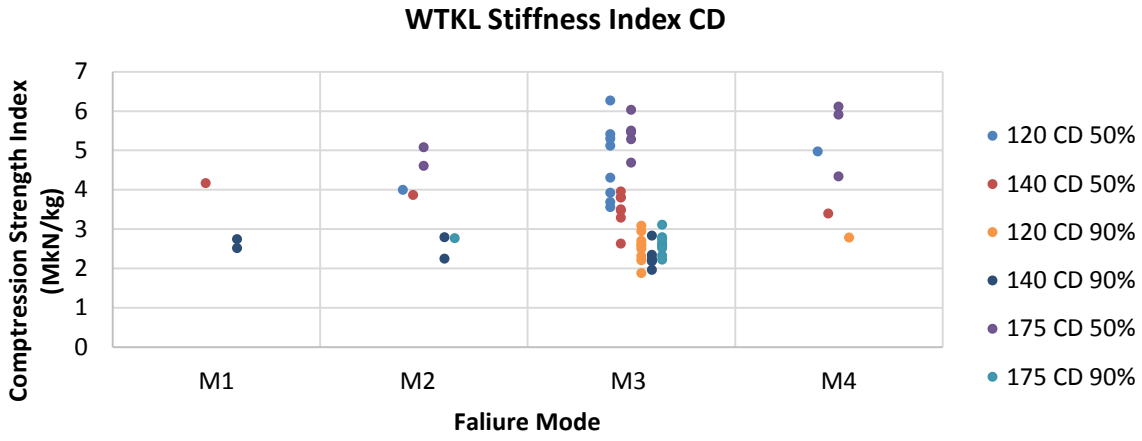

Figure A-III. 18

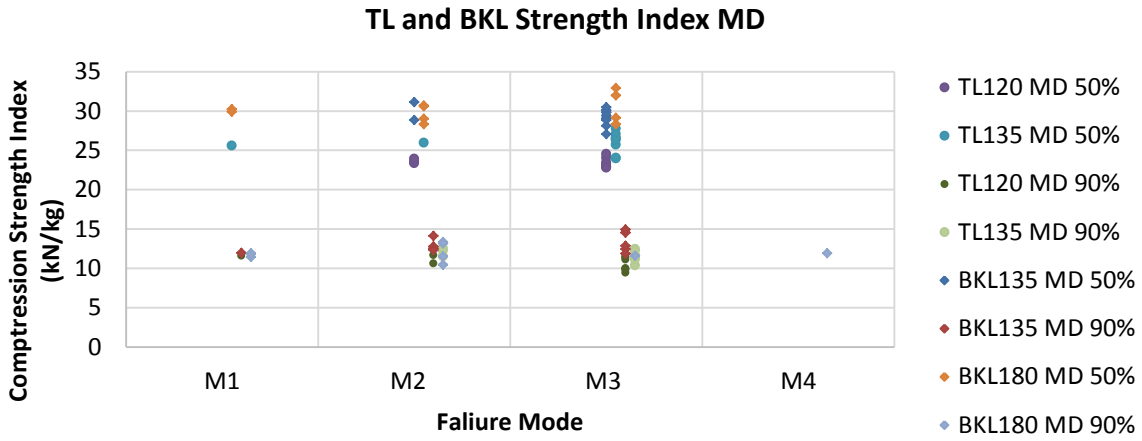

Figure A-III. 19

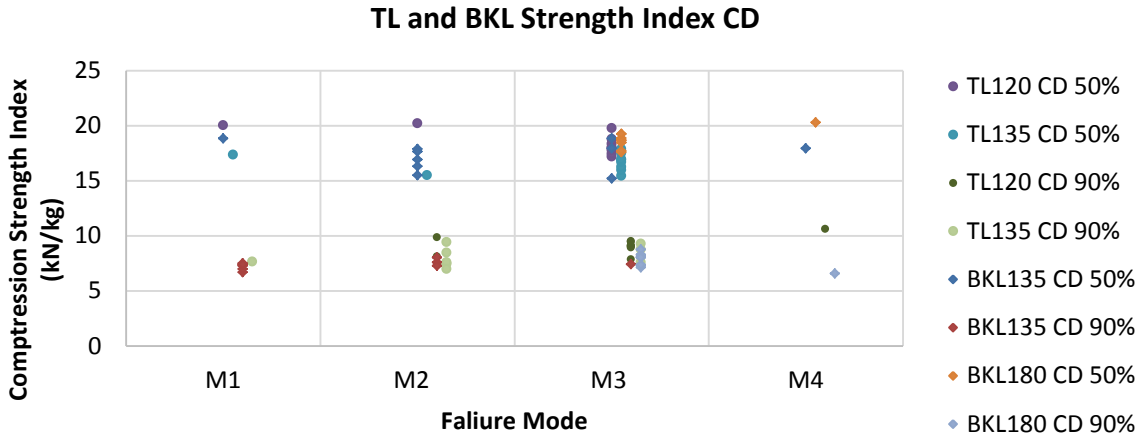

Figure A-III. 20

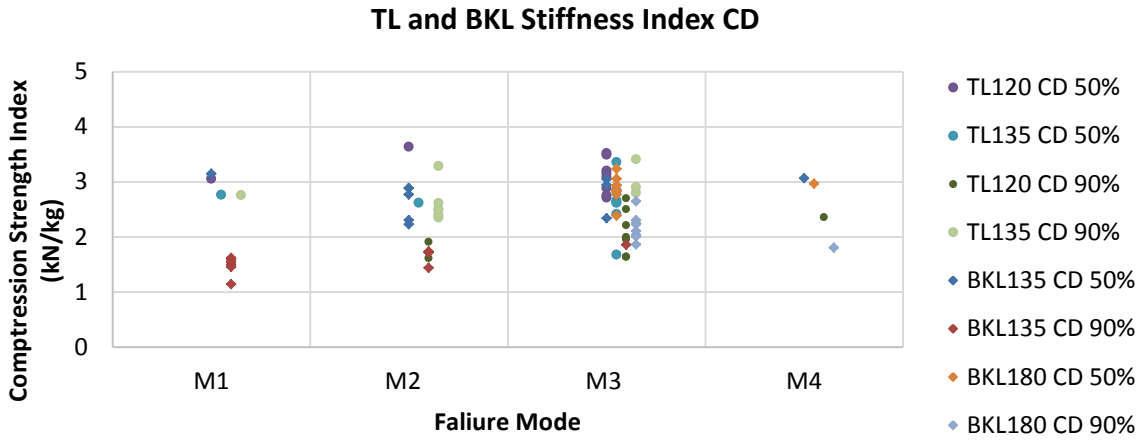

Figure A-III. 21

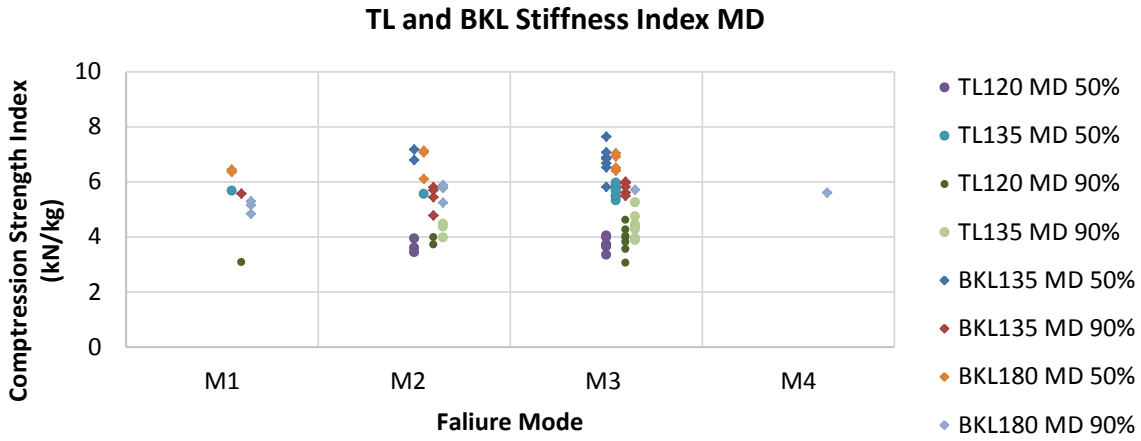

Figure A-III. 22

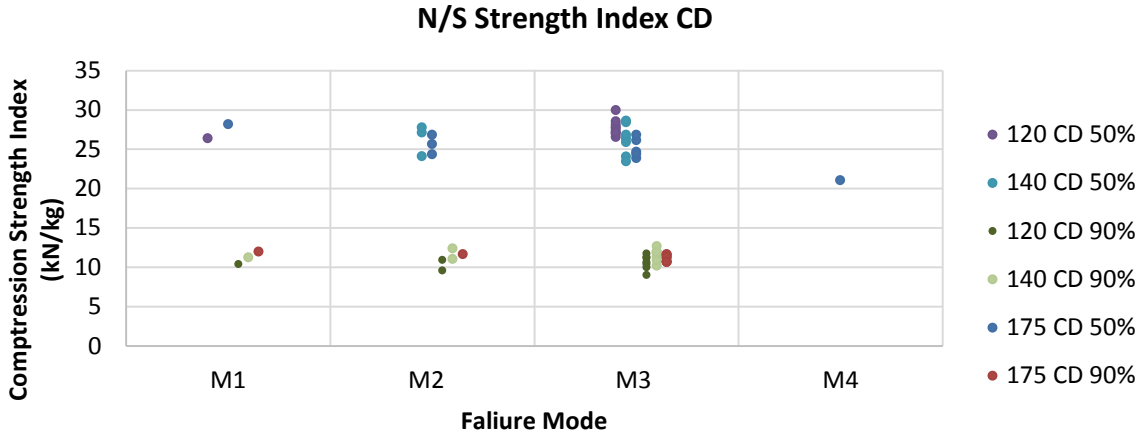

Figure A-III. 23

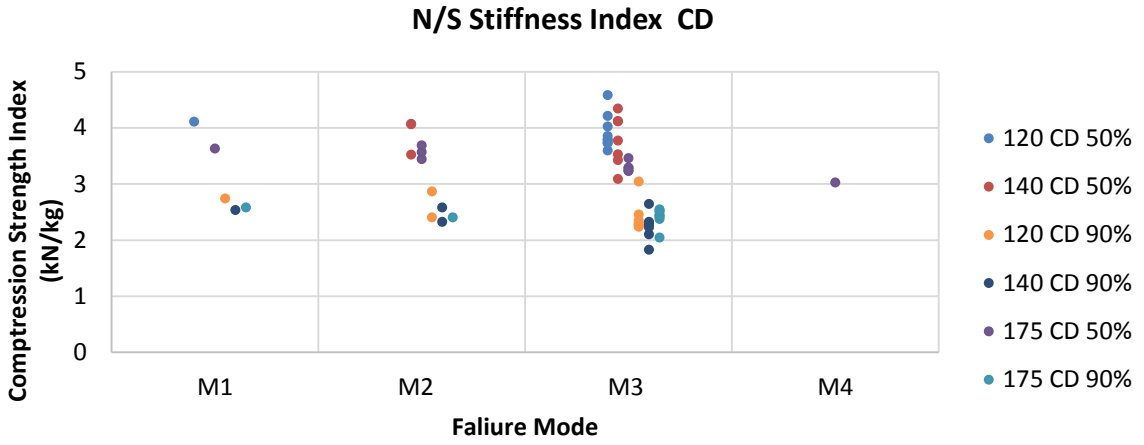

Figure A-III. 24

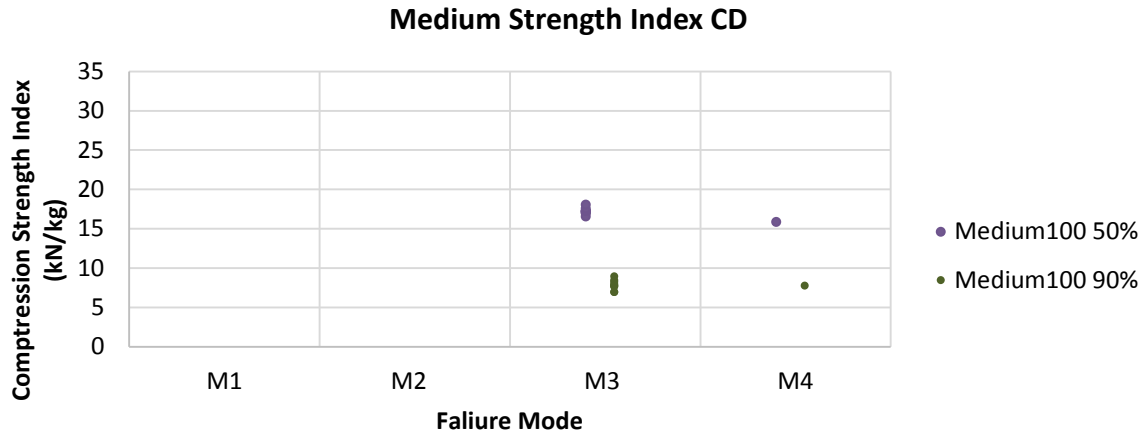

Figure A-III. 25

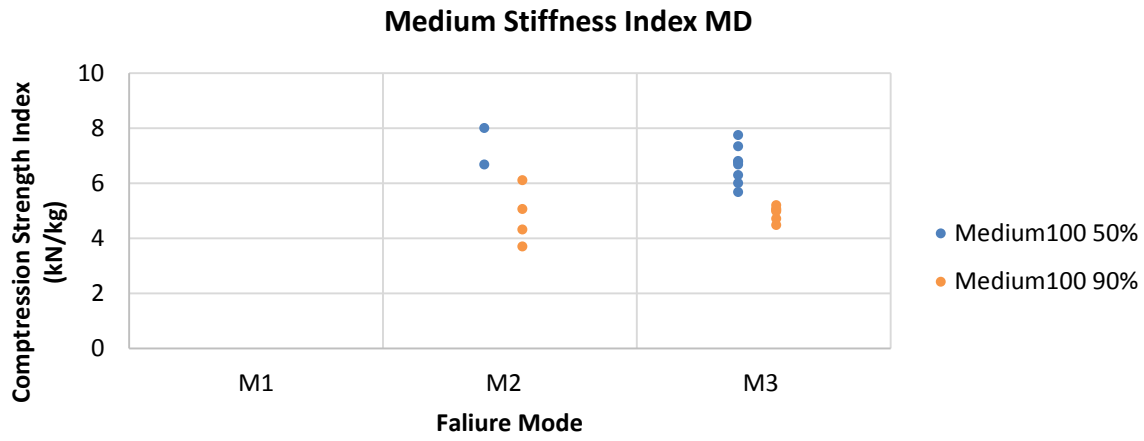

Figure A-III. 26

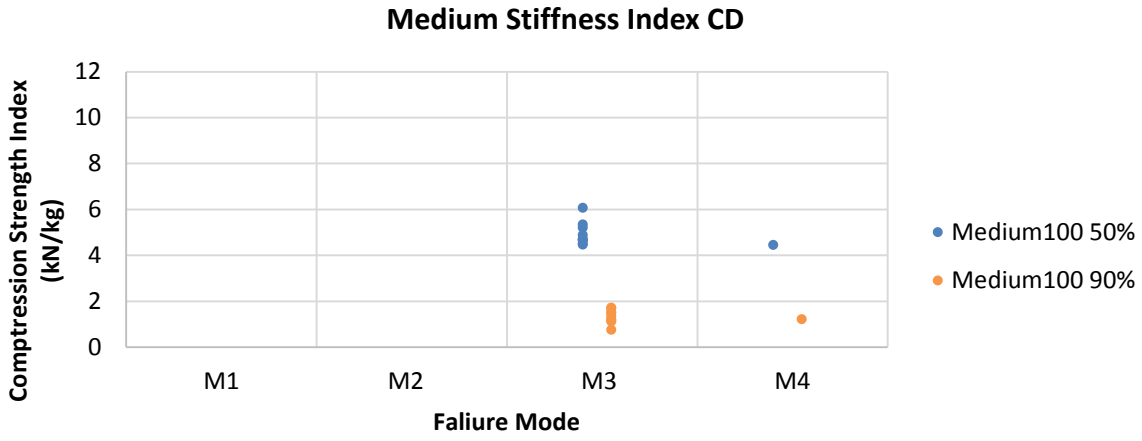

Figure A-III. 27

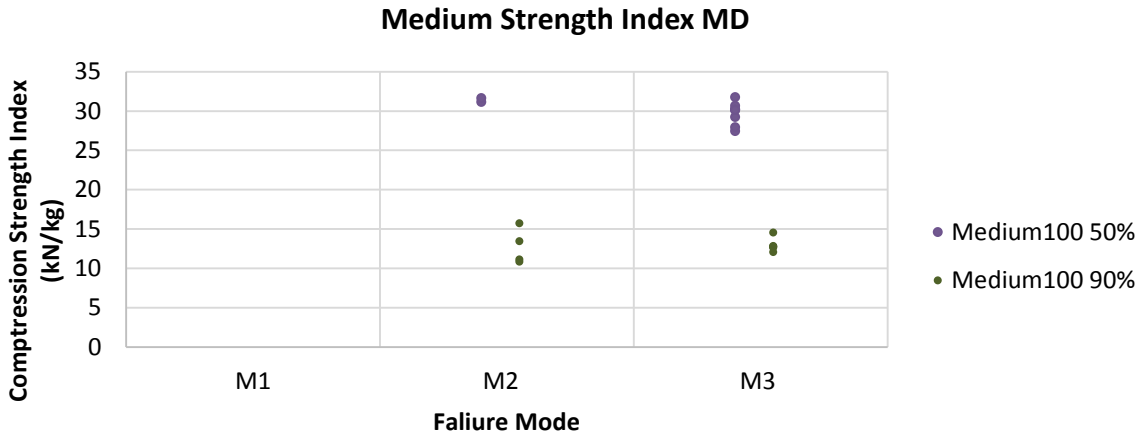

Figure A-III. 28